MODIS DAILY PHOTOSYNTHESIS (PSN) AND ANNUAL NET PRIMARY PRODUCTION (NPP) PRODUCT (MOD17)

Algorithm Theoretical Basis Document

Version 3.0
29 April 1999

Investigators:
Steven W. Running (Principal Investigator)
Ramakrishna Nemani (Associate Investigator)
Joseph M. Glassy (Software Engineer)
Peter E. Thornton (Research Associate)

Table of Contents

1. INTRODUCTION

1.1 Identification

MODIS Product No. 17 (MOD17)			
Parameter number	Parameter Name	Spatial Resolution	Temporal Resolution
3716	Photosynthesis (PSN)	1km	8-day
2703	Net Primary Production (NPP)	1km	annual

1.2 Overview

Probably the single most fundamental measure of "global change" of practical interest to humankind is change in terrestrial biological productivity. Biological productivity is the source of all the food, fiber and fuel that humans survive on, so defines most fundamentaly the habitability of the Earth.

The spatial variability of NPP over the globe is enormous, from about 1000 gC/m^2 for evergreen tropical rain forests to less than 30 gC/m^2 for deserts (Lieth and Whittaker 1975). With increased atmospheric CO_2 and global climate change, NPP over large areas may be changing (Myneni et al 1997a, VEMAP 1995, Melillo et al 1993).

Understanding regional variability in carbon cyle processes requires a dramatically more spatially detailed analysis of global land surface processes. Beginning in summer 1999, the NASA Earth Observing System will produce a regular global estimate of near-weekly photosynthesis and annual net primary production of the entire terrestrial earth surface at 1km spatial resolution, 150 million cells, each having PSN and NPP computed individually.

The PSN and NPP products are designed to provide an accurate, regular measure of the production activity or growth of terrestrial vegetation. These products will have both theoretical and practical utility. The theoretical use is primarily for defining the seasonally dynamic terrestrial surface CO_2 balance for global carbon cycle studies such as answering the "missing sink question" of carbon (Tans et al. 1990). The spatial and seasonal dynamics of CO_2 flux are also of high interest in global climate modeling, because CO_2 is an important greenhouse gas (Keeling et al. 1996, Hunt et al 1996).

Currently, global carbon cycle models are being integrated with climate models, towards the goal of integrated Earth Systems Models that will represent the dynamic interaction between the atmosphere, biosphere and oceans. The weekly PSN product is most useful for these theoretical CO_2 flux questions.

The practical utility of these PSN/ NPP products is as a measure of crop yield, range forage and forest production, and other economically and socially significant products of vegetation growth. The value of an unbiased, regular source of crop, range and forest production estimates for global political and economic decision making is immense. These products will be available for all users worldwide. This daily computed PSN more correctly defines terrestrial CO_2 fluxes than simple NDVI correlations currently done to increase understanding on how the seasonal fluxes of net photosynthesis are related to seasonal variations of atmospheric CO_2.

2. THEORETICAL BACKGROUND

2.1 Estimating NPP from APAR

The notion of a conservative ratio between absorbed photosynthetically active radiation (APAR) and net primary production (NPP), was proposed by Monteith (1972; 1977). Monteith's original logic suggested that the NPP of well-watered and fertilized annual crop plants was linearly related to the amount of solar energy they absorbed. APAR depends on the geographic and seasonal variability of daylength and potential incident radiation, as modified by cloudcover and aerosols, and on the amount and geometry of displayed leaf material. This logic combined the meteorological constraint of available sunlight reaching a site with the ecological constraint of the amount of leaf-area absorbing that solar energy, avoiding many complexities of carbon balance theory.

Time integrals of APAR have been shown to correlate well with observed NPP (Asrar et al., 1984; Goward et al., 1985; Landsberg et al., 1996), but different relationships are observed for different vegetation types, and for the same vegetation type under different growth conditions (Russell et al., 1989). Other factors influencing NPP, in addition to APAR, include: concentration of photosynthetic enzymes (Evans, 1989; Ellsworth and Reich, 1993; Hirose and Werger, 1994; Reich et al., 1994; Reich et al., 1995); canopy structure and average PAR flux density (Russell et al., 1989; Beringer, 1994); respiration costs for maintenance and growth (Lavigne and Ryan, 1997; Maier et al., 1998); canopy temperature (Schwarz et al., 1997); evaporative demand (Meinzer et al., 1995; Dang et al., 1997; Pataki et al., 1998); soil water availability (Jackson et al., 1983; Davies and Zhang, 1991; Will and Teskey, 1997); and mineral nutrient availability (Fahey et al., 1985; Aber et al., 1991; Hikosaka et al., 1994). The challenge of estimating NPP from APAR over a global domain is in accounting for these multiple influences.

Although it has been clearly demonstrated that useful empirical relationships between measured NPP and measured APAR can be derived for individual sites or related groups of sites, the objective parameterization of these empirical relationships over the global range of climate and vegetation types is a more difficult problem. Monteith's original formulation included a maximum radiation conversion efficiency (ε_{max}) that was attenuated by the influence of other simple environmental factors postulated to reduce growth eficiency. The same basic approach has been used in most other applications of the radiation use efficiency concept, with the most significant differences between approaches being the determination of values for ε_{max} and the functional forms for its attenuation. Early applications assumed a universal constant for ε_{max} that would apply across vegetation types, but later studies showed important differences in maximum efficiency between types (Russell et al., 1989). It has been shown that differences in autotrophic respiration costs may account for some of the important differences in ε_{max} between vegetation types (Hunt, 1994), which suggests that APAR may be more closely related to the gross primary production (GPP) than to NPP (GPP is the photosynthetic gain before any plant respiration costs have been subtracted). This approach, using APAR to predict GPP instead of NPP, and later accounting for respiration costs through other relationships, has been employed in recent studies (Prince and Goward, 1995). Since the relationships of environmental variables, especially temperature, to the processes controlling GPP and those controlling autotrophic respiration have fundamentally different forms (Schwarz et al., 1997; Maier et al., 1998),

it seems likely that the empirical parameterization of the influence of temperature on production efficiency would be more robust if the gross production and autotrophic respiration processes were separated. This is the approach we employ in the MOD17 algorithm.

2.2 Relating APAR and surface reflectance

A strong relationship has been shown to exist for vegetated surfaces between the fractional absorption of incident PAR and the surface reflectance of incident radiation (Sellers, 1987; Asrar et al., 1992). A robust predictive theory for this relationship has also been established (Sellers et al., 1992). This relationship makes the radiation conversion efficiency logic an attractive avenue for predicting NPP from remote sensing inputs (Prince, 1991; Potter et al., 1993; Prince and Goward, 1995; Hunt et al., 1996; Veroustraete et al., 1996; Hanan et al., 1997).

It is important to note that the radiation use efficiency logic requires an estimate of APAR, while the usual application of remote sensing data provides an estimate of FPAR, the fraction of incident PAR that is absorbed by the surface (APAR = PAR * FPAR). Measurements or estimates of PAR are therefore required in addition to the remotely sensed FPAR. For studies over small spatial domains with in situ measurement of PAR at the surface, the derivation of APAR from satellite-derived FPAR is straightforward. Implementation of the radiation use efficiency logic for the MODIS NPP algorithm depends on global daily estimates of PAR, ideally at the same spatial resolution as the remote sensing inputs, which is a challenging problem. Various methods have been implemented to address this problem, and we will consider some of them in a later section. For now, we simply note that in spite of the strong theoretical and empirical relationship between remotely sensed surface reflectance and FPAR, accurate estimates of NPP will depend at least as strongly on the quality of the global daily estimates of PAR.

3. ALGORITHM OVERVIEW

This section outlines the logic of the MOD17 PSN/NPP algorithm, addressing the science issues that have guided its development and implementation. Section 4 addresses the parameterization of the biome properties lookup table, and Section 5 addresses the details of algorithm implementation, focusing on compute structure, data handling, processing loads, and quality assurance issues. Section 6 covers algorithm validation eforts.

The essence of the core science in the MOD17 algorithm is an application of the radiation conversion efficiency logic to predictions of daily GPP, using satellite-derived FPAR (from MOD15) and independent estimates of PAR and other surface meteorological fields (from the DAO), and the subsequent estimation of maintenance and growth respiration terms that are subtracted from GPP to arrive at annual NPP. The maintenance respiration (MR) and growth respiration (GR) components are derived from allometric relationships linking daily biomass and annual growth of plant tissues to satellite-derived estimates of leaf area index (LAI) from MOD15. These allometric relationships have been derived from extensive literature review, and incorporate the

same parameters used in the Biome-BGC ecosystem process model (Running and Hunt, 1993, Thornton et al., in prep., White et al., in prep.).

The parameters relating APAR to GPP and the parameters relating LAI to MR GR are estimated separately for each unique vegetation type in the at-launch landcover product (MOD12). The GPP parameters are derived empirically from the output of Biome-BGC simulations performed over a gridded global domain using multiple years of gridded global daily meteorological observations. The MR and GR parameters are taken directly from the Biome-BGC ecophysiological parameter lists, which are organized by plant functional type (White et al., in prep.). See Section 4 for a discussion of the parameterization process for GPP and respiration parameters.

MOD17 operates over the global set of 1km land pixels, using the combination of daily and annual processing just outlined. The discussion of daily and annual processing in the following subsections is with respect to a single 1km land pixel. Details of the treatment of gridding, tiling, and storage of intermediate variables are presented in Section 5, Algorithm Implementation.

3.1 Daily estimation of GPP

For a particular pixel from the global set of 1km land pixels, daily estimated FPAR from MOD15 and daily estimated PAR from DAO are multiplied to produce daily APAR for the pixel. Based on the at-launch landcover product, a set of radiation conversion efficiency parameters are extracted from the biome properties lookup table (BPLUT). There are five such parameters for each vegetation type:

Table 3.1 BPLUT parameters for daily GPP

parameter	units	description
ε_{max}	(kgC MJ^{-1})	the maximum radiation conversion efficiency
$TMIN_{start}$	(°C)	the daily minimum temperature at which $\varepsilon = \varepsilon_{max}$ (for optimal VPD)
$TMIN_{full}$	(°C)	the daily minimum temperature at which $\varepsilon = 0.0$ (at any VPD)
VPD_{start}	(Pa)	the daylight average vapor pressure deficit at which $\varepsilon = \varepsilon_{max}$ (for optimal TMIN)
VPD_{full}	(Pa)	the daylight average vapor pressure deficit at which $\varepsilon = 0.0$ (at any TMIN)

The two parameters for TMIN and the two parameters for VPD are used to calculate two scalars that attenuate ε_{max} to produce the final ε used to predict GPP. These attenuation scalars are simple linear ramp functions of daily TMIN and VPD, as illustrated for TMIN in the following figure:

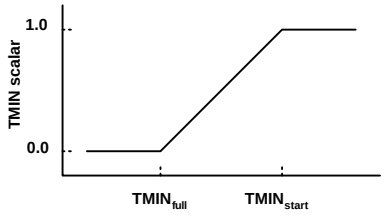

The final estimation of daily GPP is illustrated in the top panel of Figure 3.1, below.

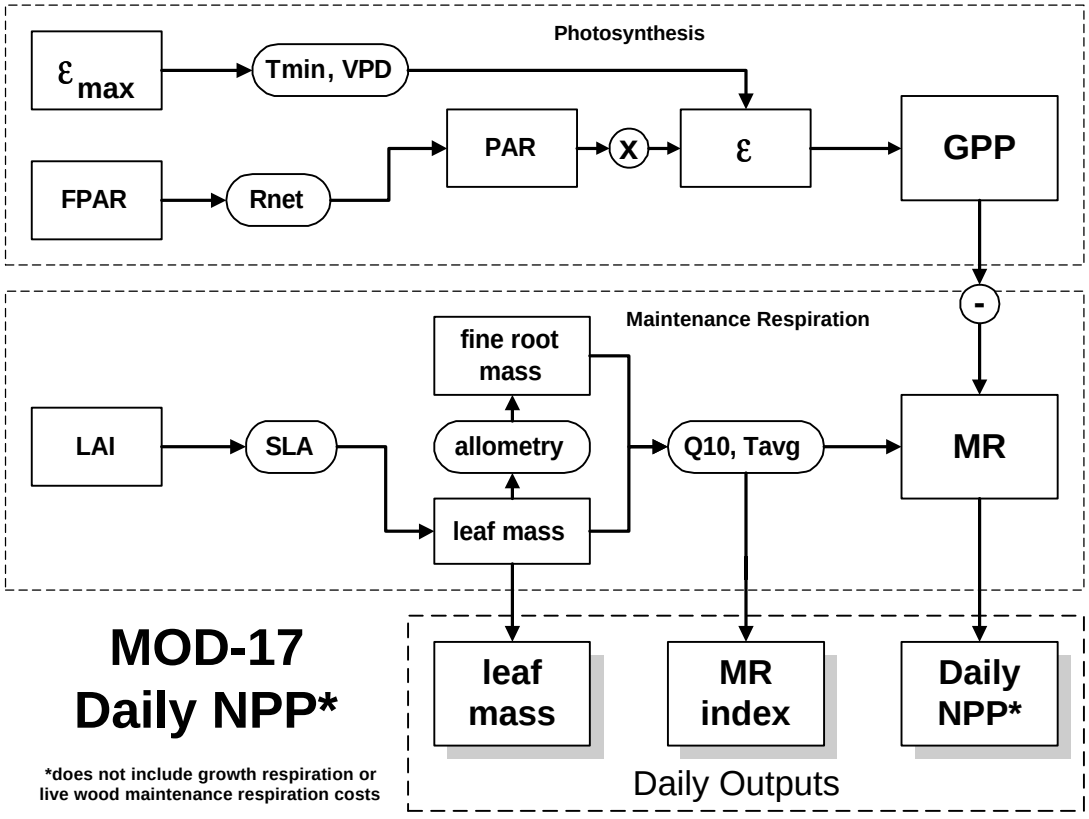

Figure 3.1 This flowchart illustrates data flow in the daily part of the MOD17 algorithm. Output variables are shown at the bottom, where the notation NPP* indicates that not all of the autotrophic respiration terms have been subtracted. The remaining terms required to produce actual NPP are handled in the annual timestep.

The second step of the daily process is to estimate maintenance respiration costs for leaves and fine roots. These estimates are based on a standard exponential function of daily average air temperature (Sprugel et al., 1995; Ryan et al., 1997; Maier et al., 1998), scaled by the biomass of leaves and fine roots. We use LAI from MOD15 to estimate leaf mass, based on a specific leaf area (SLA) from the BPLUT. Fine root mass is assumed to be present in a constant ratio to leaf mass. This process is illustrated in the center panel of Figure 3.1. The following parameters from the BPLUT are required for these calculations:

Table 3.2 BPLUT parameters for daily MR

parameter	units	description
SLA	(m^2 kgC^{-1})	projected leaf area per unit mass of leaf carbon
froot_leaf_ratio	none	ratio of fine root carbon to leaf carbon
leaf_mr_base	kgC kgC^{-1} day^{-1}	maintenance respiration per unit leaf carbon per day at 20°C
froot_mr_base	kgC kgC^{-1} day^{-1}	maintenance respiration per unit fine root

		carbon per day at 20°C
q10_mr	none	exponent shape parameter controlling respiration as a function of temperature

There are several components of the plant respiration costs that cannot be estimated accurately on each daily timestep, given the constraints of the data available in the MODIS processing stream. One of these is the component of maintenance respiration in woody vegetation types that is due to the live cells of the woody biomass. These cells are present and respiring as a function of temperature throughout the year, even for deciduous types which have no leaves displayed in the winter or drought months. The logic used above to relate fine root mass to leaf area will not work for this component, since it misses respiration occurring when the trees are bare. A better approach is to assume that the amount of live woody tissue is constant through the year, and is related to the annual maximum leaf mass. By sending daily leaf mass as an output from the daily algorithm, this annual maximum can be assessed in the annual timestep logic. Because of the non-linear influence of temperature on maintenance respiration, it is also necessary to send an index of daily maintenance respiration potential as an output from the daily algorithm, so that once the live woody tissue mass is known it can be used to estimate annual total live woody maintenance respiration.

Growth respiration is the other component that cannot be estimated accurately at the daily timestep, since the daily estimates of LAI provided by MOD15 do not necessarily correspond to any particular growth rate. Differencing of LAI between timesteps could possibly produce estimates of daily growth, but such a method would be very sensitive to random variation in estimated LAI. Here again we use the annual maximum of leaf mass, together with empirical allometric relationships estimated from literature review, to estimate growth and its associated respiration costs. The daily output of leaf mass described above is used for this purpose.

Since some of the maintenance respiration costs and all of the growth respiration costs have not been accounted for in the daily timestep, the daily output from this algorithm is termed NPP*, to differentiate it from the true daily NPP, which is never known. Outputs from the daily algorithm, NPP*, daily leaf mass, and an index of daily maintenance respiration, are illustrated in the bottom panel of Figure 3.1.

3.2 Annual estimation of NPP

Given outputs from the daily algorithm as specified in the previous section, the annual algorithm finishes the estimation af annual NPP by first estimating the live woody tissue maintenance respiration, then estimating the growth respiration costs for leaves, fine roots, and woody tissue. Finally, these components are subtracted from the accumulated daily NPP* to produce the an estimate of annual NPP. Figure 3.2 illustrates the flow of information in the annual algorithm.

As shown in Figure 3.2, the annual maximum leaf mass, as estimated from the output of daily leaf mass, is the primary input for estimates of both live wood maintenance respiration and whole-plant growth respiration. This approach relies on empirical studies relating annual growth of leaves to annual growth of other plant tissues. The compilation of forest biomass and primary production data by Cannell (1982) is one excellent example of the literature surveys required to establish these empirical

relationships. In addition to the annual maximum leaf mass, an estimate of leaf longevity (the inverse of leaf turnover rate) is required to predict the annual leaf growth for evergreen types. For deciduous types, leaf longevity is assumed to be less than one year, so the total leaf mass must be grown each year. Our logic makes the assumption that no litterfall begins for deciduous tyupes until the maximum annual leaf mass has been attained. In cases where litterfall is happening at the same time as new leaf growth our method would tend to underestimate the total annual growth respiration costs. The same problem applies to evergreen canopies, but with longer leaf lifespans the potential error is smaller. The following table lists the BPLUT parameters required in the annual algorithm:

Table 3.3 BPLUT parameters for annual MR and GR

parameter	**units**	**description**
livewood_leaf_ratio	none	ratio of livewood carbon to annual maximum leaf carbon
livewood_mr_base	(kgC kgC^{-1} day^{-1})	maintenance respiration per unit live wood carbon per day at 20°C
leaf_longevity	(yrs)	average leaf lifespan
leaf_gr_base	(kgC kgC^{-1})	respiration cost to grow a unit of leaf carbon
froot_leaf_gr_ratio	none	ratio of fine root to leaf annual growth respiration
livewood_leaf_gr_ratio	none	ratio of livewood to leaf annual growth respiration
deadwood_leaf_gr_ratio	none	ratio of deadwood to leaf annual growth respiration

Growth respiration costs depend only on the amount of tissue grown and the type of tissue. Although our implementation of the annual algortihm leaves open the possibility of having different growth costs for different tissues, our current implementation uses the same growth cost per unit of new carbon in leaves, fine roots, live wood, and deadwood (Larcher, 1995; Thornton, 1998). The annual algorithm uses annual maximum leaf mass and the leaf longevity to assess leaf growth respiration, and then uses empirical coefficients to relate annual leaf growth respiration costs to annual fine root, live wood, and dead wood growth respiration. These parameters are calculated directly from similar parameters used in the Biome-BGC model (White et al., in prep., Thornton et al., in prep.).

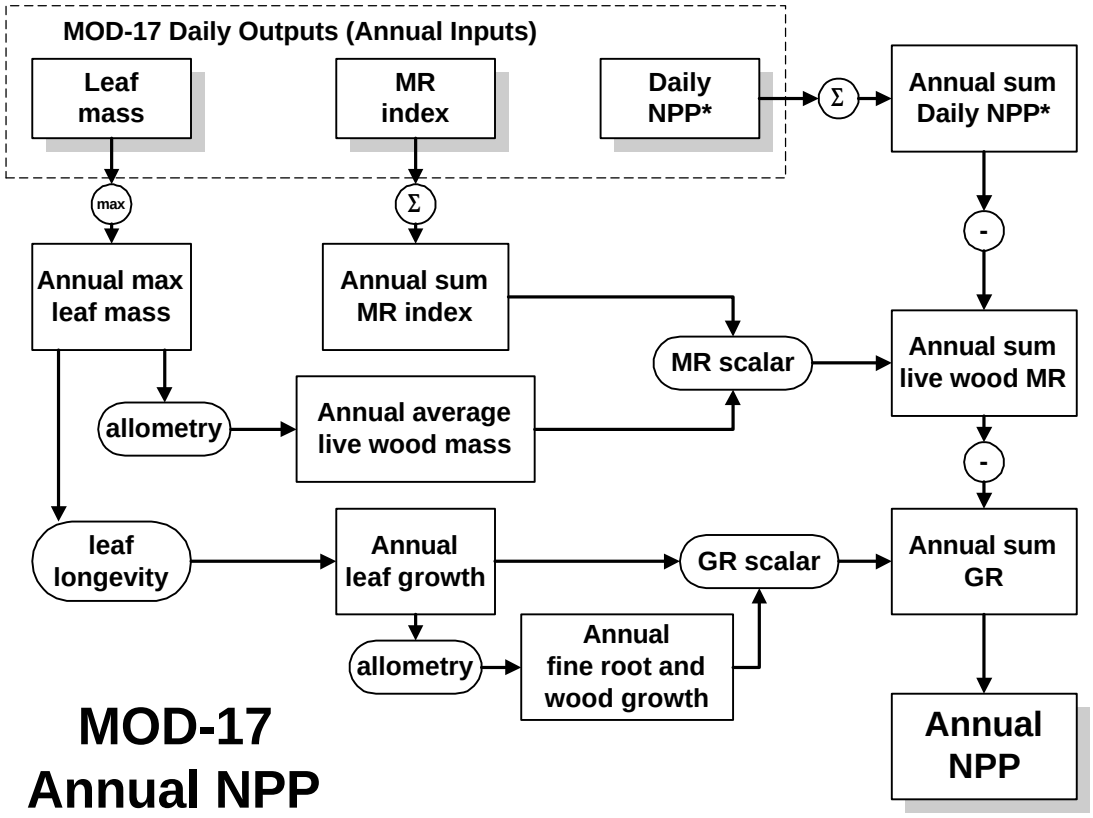

Figure 3.2 This flow chart illustrates data flow in the annual part of the MOD17 algorithm. Inputs from the daily timestep process are shown at top left. Here the remaining autotrophic respiration terms are taken into account, resulting in an estimate of annual NPP.

4. BPLUT PARAMETERIZATION

4.1 Parameterization strategy overview

Parameter values for the daily and annual algorithms all come, directly or indirectly, from the terrestrial ecosystem process model Biome-BGC. In the case of the parameters controlling daily estimates of GPP, there is an indirect connection to Biome-BGC, where daily output from extensive simulations over the global range of vegetation and climate is used to guide the parameter selection through a multivariate optimization procedure. In the case of the parameters for daily leaf and fine root maintenance respiration the parameters come directly from the model's ecophysiological parameter files that define differences between plant functional types. In the case of the annual growth respiration parameters, several Biome-BGC ecophysiological parameters are combined to calculate new parameters for the MOD17 logic.
type.

Our use of one model to parameterize another model warrants some discussion. The objective of MOD-17 is to produce accurate estimates of annual NPP for the globe, and also to provide accurate estimates of the seasonal development of annual NPP patterns for comparison to long-term normal patterns. From the conception of the

radiation conversion efficiency approach it has been recognized that the relationship between APAR and NPP (or GPP) is not simple or linear, but that it can under certain conditions provide robust empirical estimates. The strongest argument for its application in the MODIS processing stream is the direct link it provides to remotely sensed surface reflectances. This link permits estimates of NPP that account for observed landcover changes. Earlier arguments for the RUE approach focused on the lack of mechanistic understanding of terrestrial primary production, which prevented robust applications of more process-oriented approaches. Given the strong predictive ability of our mechanistic NPP algorithms, demonstrated in comparisons against measurements at multiple scales and in multiple biomes(Running, 1994; Kimball et al., 1997b; Cienciala et al., 1998; White et al., 1998), it appears that understanding of mechanism is not a serious limitation. The cost of implementing more mechanistic models in the operational MODIS processing stream is, however, an important consideration. The memory and processing requirements for Biome-BGC compared to MOD-17, for example, are on the order of 100:1, a strong argument for the radiation conversion efficiency approach.

Validation of the MOD-17 results is an important component of our research efforts, and the large number of dependencies in this level 4 product make that a very challenging process. A direct validation of the MOD-17 results with surface observations will be very difficult, and will have to wait until there is an adequate overlap between MODIS processing and surface data collection (see Section 6). There are important steps that can be taken before then, and our use of the Biome-BGC model results in parameterizing MOD-17 is an integral part of our pre-launch validation planning.

If we assume, for the moment, that the daily GPP predictions from Biome-BGC are perfect representations of real GPP under the given boundary conditions, and if we then set about parameterizing the MOD-17 algorithm to reproduce those results as closely as possible, there will still be error associated with the empirical formulation, since it is known that the MOD-17 relationships are only approximations to the processes represented more explicitly in Biome-BGC. In the process of estimating the MOD-17 parameters we are able to characterize this source of error very accurately.

Although the end result of the optimization process is a single set of parameters for each of the at-launch vegetation types, we are able to estimate the spatial and temporal patterns of error associated with the translation from Biome-BGC to MOD-17. We do not, of course, make the assumption that the Biome-BGC results are correct. Independent of the assessment of translation errors from Biome-BGC to MOD-17, we are assessing the spatial and temporal patterns of error in the Biome-BGC results when compared to observations of NPP at multiple spatial and temporal scales. The point of this discussion is that both of these sources of error need to be characterized. The use of Biome-BGC as an intermediate step between surface observations and the empirical MOD-17 algorithm simplifies the process. To understand why, consider that most of the surface observations of NPP that are currently available for model validation do not characterize FPAR or LAI, both of which are essential inputs to the MOD-17 algorithm. Biome-BGC treats FPAR and LAI and prognostic variables as opposed to model constraints, and so comparisons between Biome-BGC and surface observations are more straightforward than comparisons between MOD-17 predictions and the same observations.

4.2 Parameters for daily GPP

Values for the five parameters listed in Table 3.1 are determined through a multivariate optimization process which minimizes the mean absolute error in daily GPP as predicted by MOD-17 compared to the daily estimates of GPP from a global application of the Biome-BGC model. Optimization is by the downhill simplex method of Nelder and Mead, as described in Press et al. (1992). The downhill simplex method was chosen for its robust behavior when the function being minimized is not smooth, as is the case for the MOD-17 GPP algorithm.

The foundation of this parameterization process is a set of simulations performed with the Biome-BGC model over a global grid (1° x 1°) using daily meteorological data from Piper (1995), an aggregated version of the 1 km at-launch landcover product, and additional 1km landcover information from the University of Maryland describing the fractional cover of woody vegetation by leaf type and leaf duration. Outputs from these simulations included daily GPP, LAI, and FPAR. These outputs were used in conjunction with the daily meteorological data to diagnose empirical relationships between APAR and GPP for each vegetation type.

The following sections provide an overview of the Biome-BGC model logic as it pertains to the MOD17 BPLUT parameters for GPP, and a description of the model simulations used to produce the at-launch BPLUT values.

4.2.1 Biome-BGC model overview

The Biome-BGC model predicts the states and fluxes of water, carbon, and nitrogen in a system including vegetation, litter, soil, and the near-surface atmosphere. For the purposes of parameterizing the MOD17 GPP BPLUT values, the most relevant parts of Biome-BGC are the components concerned with daily predictions of gross photosynthesis. While it is possible to consider the details of single or several model components in isolation, the full dynamics of the model are not realized unless all the components of the water, carbon and nitrogen budgets are operating together. It is the complex interactions between these cycles and the physical driving variables that make a process-based model such a useful investigative tool.

The interactions between the carbon and water budgets of the Biome-BGC model have been described in considerable detail elsewhere (Running, 1984; Running and Coughlan, 1988; Running et al., 1989; Running and Hunt, 1993; Kimball et al., 1997c). Much of the mechanism representing the interaction between the carbon and nitrogen cycles has not been explored in other publications. Figure 4.1 illustrates the model's major pathways for carbon and nitrogen transport, and also shows some points of control between the two cycles. Of particular relevance for the MOD17 logic is the connection between the carbon and nitrogen cycles in the allocation logic. Carbon and nitrogen allocation is controlled by fixed C:N ratios, so new growth is dependent on there being an adequate supply of both C, from the gross photosynthesis process, and N, taken up by the plants from the soil mineral N pool. In the case of excess C coming from the photosynthesis predictions, with respect to the N available from the soil mineral N pool, gross photosynthesis is reduced, effectively attenuating the nitrogen use efficiency under N-limiting conditions.

The implication of this interaction for MOD17 parameterization is that in addition to the direct environmental controls on photosynthesis that influence the radiation

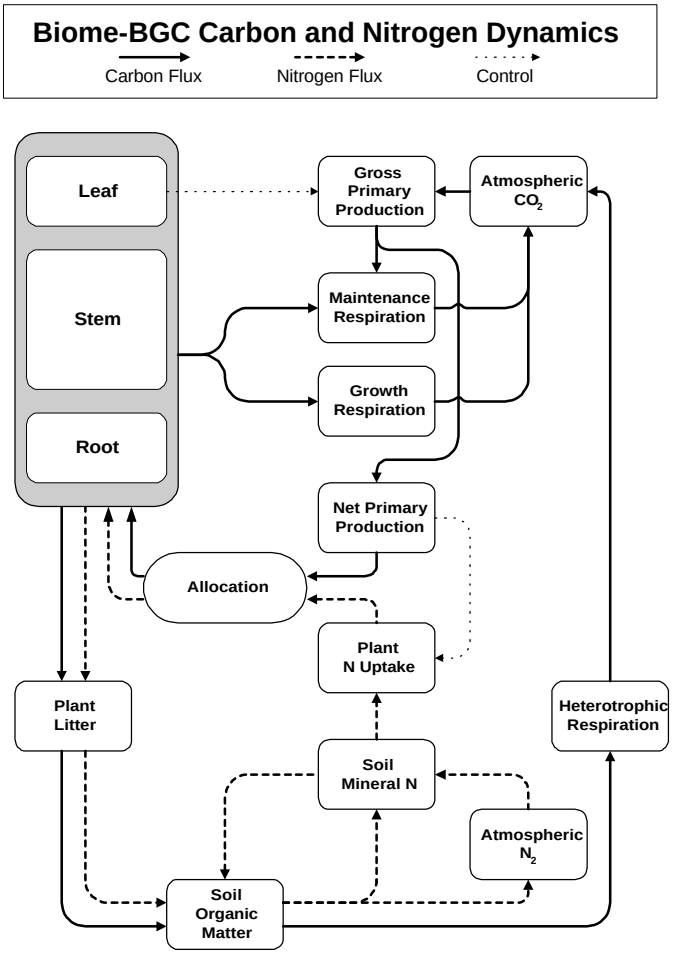

Figure 4.1 This flow chart illustrates some of the most important fluxes of carbon and nitrogen within the plant-litter-soil-atmosphere system, as represented by the Biome-BGC model.

conversion efficiency relationship, there are indirect controls that operate through the influence of environmental conditions on the mineralization of N from decomposing litter and soil organic matter (Figure 4.2). These influences appear in the daily GPP outputs, and can be at least partly captured in the estimates of ε_{max} derived from those outputs.

In addition to the influences of environmental factors on the internal cycling of carbon and nitrogen between plants, litter, and soil organic matter, there are strong interactions between disturbance processes and the inputs and outputs of carbon and nitrogen to and from the plant-litter-soil system. For example, fire consumes organic matter and releases CO_2 to the atmosphere, but it also can either volatilize or release in mineral form the nitrogen originally associated with the consumed organic matter. The cumulative effects of these infrequent events on the mineral nitrogen pool available for new plant growth can be very large, and the degree of influence varies with climate and with fire frequency and intensity. Biome-BGC includes a parameterization of fire frequency and intensity, and the long-term steady-state reached between climate and soil organic matter is sensitive to the nature of this parameterization. These are influences that can only be roughly captured through the empirical radiation conversion efficiency logic, since there is no explicit treatment of disturbance regimes. The ability to capture at least some of this variation is an argument in favor of our approach to estimating the GPP parameters.

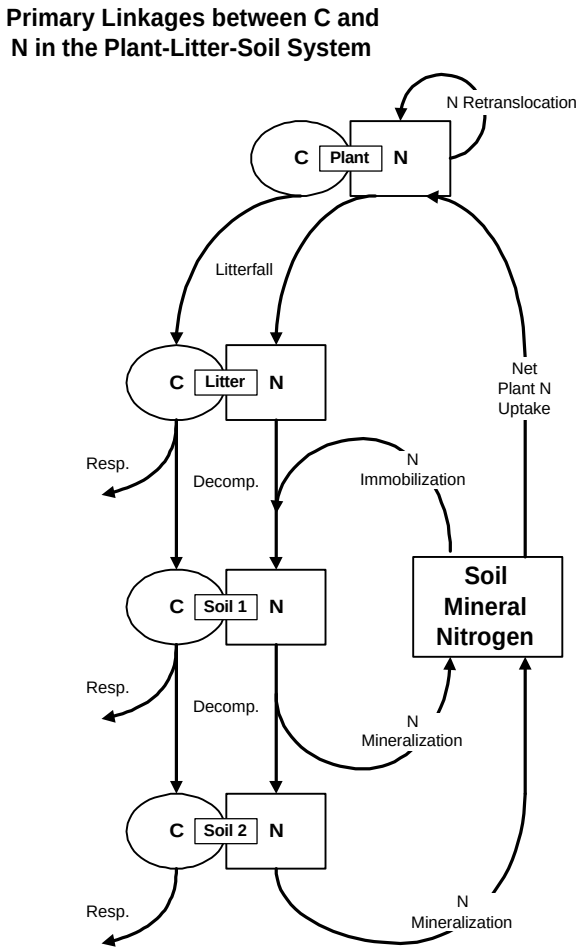

Figure 4.2 This flowchart shows the interactions between plant litterfall, litter decomposition to soil organic matter, and the internal cycling of N back to the plant as soil organic matter loses CO_2 as the result of heterotrophic respiration.

4.2.2 Experimental protocol for global simulations

The objective of the MOD17 GPP prediction strategy is to capture as much as possible of the complex dynamics of Biome-BGC's predictions of GPP in a simple empirical structure. In order to do this, it is necessary to perform a set of functionally complete simulations and then analyze the resulting daily outputs.

In order to capture as much of the global range of variation in climate and landcover as possible, we performed gridded daily simulations over a global 1°x1° grid. Meteorological input was from the 14-year daily dataset developed at Scripps Oceanographic Institute (Piper, 1995). Gridded soil physical parameters were estimated from the Zobler soil texture database (Zobler, 1986). Landcover data was obtained from researchers at the Laboratory for Global Remote Sensing Studies at the University of Maryland. This consisted of two separate datasets: a discrete classification that is also the at-launch MODIS landcover product, and a continuous fields product that describes the fractional cover of woody species in each grid cell, and also discriminates woody cover fraction down by leaf longevity and leaf morphology. Both these datasets are on a 1km grid. We combined the two in order to arrive at a description of plant functional type suitable for the Biome-BGC model that also agreed with both the discrete and continuous classifications provided by UMD. This new 1km product was aggregated to a 1°x1° grid, preserving the fractional cover information within each gridcell. In this way, the global areal coverage of the functional vegetation types is preserved in the aggregation process, which is not the case when aggregating a discrete classification using wither the nearest neighbor or majority reclass approaches.

For each gridcell, a separate (independent) Biome-BGC simulation was performed for each functional vegetation type having greater than 1% of the total vegetated land area within the cell. Types with less than 1% cover (taken as a percent of the total vegetated land area in the cell) were ignored for these simulations, and their

weight was distributed among the remaining vegetation types according to their relative areas.

The Scripps meteorological dataset contains 14 years of daily gridded surfaces for maximum and minimum temperature and precipitation. We used these variables to estimate daily humidity (Kimball et al., 1997a) and radiation (Thornton and Running, 1999). over the grid. Daylength was calculated for each grid cell from standard geometric relationships.

Soil carbon and nitrogen approach steady-state values with respect to climate over the course of hundreds to thousands of years in these simulations. Because of the strong dependence of plant carbon and nitrogen allocation on soil mineral nutrition status, and because this dependency translates to variation in optimized parameters for the radiation conversion efficiency logic, it was necessary to perform model spinup runs that allowed the soil organic matter and mineral nutrient pools to stabilize. Our approach was to start all soils with no organic matter, and plants with a very low initial biomass, and let the soil organic matter and plant biomass agrade over many cycles through the 14-year daily driver record. We find that the timespans for spinup depend very strongly on the rates of exogenous nitrogen deposition and the counteracting rates loss through leaching, denitrification, and volatilization from fire. We also found that the same final system-wide steady states could be reached by either maintaining a slow and constant rate of nitrogen deposition (wet+dry) characteristic of pre-industrial conditions, or by alternating high and low nitrogen deposition periods, monitoring the changes in soil organic matter over hundres of simulation years between pulses of high deposition to assess the approach to a steady-state. The simulations using pulses N deposition reached a steady-state in about 20% of the number of years required for the steady N deposition runs. This is the most time intensive part of the simulations, and so savings of 80% are significant.

The steady-state for each vegetation type in each cell is monitored independently, so a different number of spinup years is required for different cells. Once the steady state is reached, defined by a variation in total soil carbon averaged over several hundred years of less than 0.001%/yr, a restart record is written so that the simulation can be started again from the steady-state point without having to repeat the lengthy spinup period.

These spinup runs describe a hypothetical global steady-state for primary production (as well as net ecosystem exchange) characteristic of the preindustrial atmosphere and nitrogen cycles. Because the optimized MOD17 GPP parameters are sensitive to the soil nutrient status, anthropogenic influences on such variables as atmospheric concentrations of CO_2 and the rate of N deposition have important consequences for the MOD17 algorithm, to the extent that these factors influence soil organic matter and plant biomass states (Hudson et al., 1994; Keeling et al., 1996). For this reason, we extended the pre-industrial spinup runs into the historical record of increasing atmospheric CO_2 and atmospheric N deposition, assuming 1895 as a starting point, and following the record of CO_2 established for use in the VEMAP (VEMAP Members, 1995). We used data from the MOGUNTIA model (Dentener and Crutzen, 1994), as reported by Holland et al. (1997), to set the industrial N deposition levels (circa 1990), and scaled the historical trend of N deposition to follow the trend in atmospheric CO_2 concentration. The actual period of record for the Scripps meteorological database is 1980-1993. We ran our historical simulations from their steady-state starting point in 1895 through 1980, then performed a single 14-year simulation to capture the dynamics

in daily GPP and autotrophic respiration as responding to realistic interannual climate variability from 1980 though 1993. Due to changing atmospheric CO_2 and N deposition, this final set of simulations used for parameterizing MOD17 does not represent a steady-state response, since carbon is agrading in most systems under increased fertilization. We believe that capturing this disequilibrium state is important in making accurate global predictions of NPP. We are continuing to explore these issues. Of course, there is no influence from changing climate in these simulations, since the same 14-year record is used for the spinup period, the historical period, and the final simulation period.

4.2.3 Optimal parameter selection

Given the gridded global daily outputs for GPP and APAR from Biome-BGC over the 14-year period of record, and the accompanying meteorological data for daily minimum temperature (TMIN) and vapor pressure deficit (VPD), we used a numerical method for multivariate optimization to select parameters for the MOD17 GPP prediction algorithm that would produce GPP results as close to the Biome-BGC GPP outputs as possible. An independent optimization was performed for each vegetation type in each land grid cell, using the 14-year daily record of GPP as the minimization target.

The five parameters in Table 3.1 are the potential candidates for optimization. We found that the covariance between parameters in their relationships to GPP was such that, when all five were left unconstrained and simultaneously optimized, nearly the same minimum prediction error could be attained with very different parameter combinations. Covariance between temperature and VPD also tended to reduce the optimization efficiency, since the influence of temperature on GPP over most of the environmental temperature range is to increase productivity, while the influence of VPD, through restriction of stomatal conductance, is to decrease production. However, because temperature and VPD are strongly positively correlated, their contrasting control on GPP is difficult to assess through empirical parameter selection. By using the ecophysiological parameters from Biome-BGC that constrain the stomatal conductance response to VPD as fixed parameters in the MOD17 GPP algorithm, this covariance problem is eliminated. This approach leaves three parameters to be optimized; ε_{max}, $TMIN_{start}$ and $TMIN_{full}$. Even with only three parameters to fit, we found a strong correlation between the optimized values for ε_{max} and $TMIN_{start}$, such that higher values of ε_{max} were associated with higher values of $TMIN_{start}$, resulting in very similar patterns of GPP with very different parameter values. By further constraining the optimization so that $TMIN_{full}$ was forced to -10°C (see figure on p. 8), and fitting only ε_{max} and $TMIN_{start}$, the correlation between the fitted parameters was greatly reduced, without significant loss in prediction accuracy.

5. ALGORITHM IMPLEMENTATION

The MODIS EOS (AM-1 Terra platform) PSN and NPP land science algorithms are global scale, 1KM resolution, daily timestep ecosystem models driven from MODIS instrument data and selected ancillary datasets. Photosynthesis (PSN) is the foundation ecosystem variable computed. PSN represents plant productivity and is expressed in terms of carbon mass per unit area per day. Annual net primary productivity (NPP) is

derived directly from PSN, with the effects of maintenance respiration costs taken into account. While the PSN and NPP pixel wise measures are computed daily, the archived EOSDIS Core System (ECS) PSN product is computed once per 8-days, and the NPP product is computed once annually. The archived PSN and NPP data products are projected in the standard MODIS Land Integerized Sinuoidal (IS) tile map projection and are stored in NASA HDFEOS format files. Each processing tile represents approximately 1200 km by 1200 km land region.

5.1 Programming/Procedural Considerations

The University of Montana PSN, NPP algorithm is implemented using a hybrid first principles and empirical approach. We compute a daily PSN term using a series of forcing variables such as MODIS 8-day FPAR, LAI, and light use efficiency (epsilon), and using other biome-wise coefficients stored in a biome properties lookup table (the BPLUT). Spatially defined ancillary inputs include a daily global climatology supplied via Data Assimilation Office (DAO) assimilated datasets (http://dao.gsfc.nasa.gov). Given good quality FPAR and LAI inputs, future scientific improvements to this algorithm are anticipated when better coefficients in the BPLUT become available.

The PSN, NPP algorithm suite is functionally divided into several components. These are:

- …a ***daily*** intermediate update routine (PGE 36: MOD17A1), in which pixel-wise gross primary productivity terms are computed and stored for each day. These intermediate daily state terms are accumulated throughout an entire annual processing cycle in a tiled HDFEOS file.
- …An ***8-day compositing*** routine, where (8) contiguous daily products are composited to produce a single PSN or NPP 1KM global data product. Note that the 8-day PSN is based on the most recently calculated (e.g. accumulated) intermediate daily gross primary productivities.
- …an ***annual NPP compositing*** routine, which outputs an 1KM global annual data product, based on the (365) day accumulated sum of gross primary productivity (GPP) less maintenance respiration (gpp - rm) term.

A single software codeset is used to implement this model logic, with the daily updating logic invariant across all 3 functional components (daily, 8-day, and annual). The single MOD17A1 daily executable from this codeset is executed once per model day for each calendar day ({1..365} for normal years, {1..366} for leap years). Note that the set of (289) daily intermediate "state" files To account for the fact that a given year does not divide evenly into 8-day periods, at the end of a given year, model data from approximately 3-5 days of the subsequent year are

5.2 Production Rule Summary

A summary of how the PSN, NPP algorithm handles various temporal boundary events follows:

Table 5.1: PSN,NPP Production Rule Summary		
Mode	PCF File PSN "BOUNDARY"	Actions Taken
"first-in-year"	0	When the first day of a year is encountered, a fresh daily intermediate file is created for each of the (289) land tiles, and the daily state variables for that day are updated.
"daily updates"	1	When a given model day not associated with an 8-day boundary or annual boundary occurs, the scheduler causes the PSN and NPP daily intermediate variables to be updated, in each of the daily (289) land tiles.
"8-day output"	2	When an 8-day period boundary is encountered, the scheduler first separately executes MOD_PR17A1 in "daily update" mode, then executes the model in "8-day output" mode to produce the archive 8-day PSN (MOD17A2 ESDT).
"Annual output"	3	When an annual period boundary is encountered, the scheduler first executes MOD_PR17A1.exe in "daily update" mode, and then executes the same program in "annual output" mode to produce the archive NPP (MOD17A3 ESDT).

5.3 Implementation Software Environment

The MOD17A1 codeset was written to comply with a number of standards, and to interoperate with several supporting binary libraries. The codes are written in ANSI C and are POSIX 1.x compliant. Both daily and 8-day codes link to the mandatory NASA Software Data Production Toolkit library (SDPTK v.5.2.4), the NASA HDF-EOS library v.2.4), and our SCF API -- the MODIS-University of Montana (MUM) API v. 2.2. The table below breaks down the lines-of-code for our at-launch PSN, NPP algorithms:

Table 5.2: PSN, NPP (PGE 36,37,38) Lines-of-code (LOC) Metrics		
Code Layer	*Lines Of Code*	*Percent of Code*
MOD_PR17A1	13016	27.48 %
MUM library	34,336	72.51 %
Total, All Codes	47352	-

5.3.1 Software Design

In designing our at-launch algorithms, emphasis was placed on code robustness, reliability and maintainability. A significant fraction of the ECS production code developed at the Montana SCF rests on the common MUM API foundations. Larger amounts of code re-use generally promote life-cycle reliability in several ways: a) the total number of potential points-of-failure (system-wide) are reduced across all algorithms sharing a common foundation, and b) the life-cycle maintenance effort required to support the shared foundation (API) code is spent just once while each "client" benefits from the software services it provides.

Another common design thread running throughout our implementations is the emphasis on data-driven parameterization of the algorithm software. By "data driven" we refer to the externalization of key software inputs, to allow some revisions in program behavior without having to recompile and link the software. The Biome Properties Lookup Table (BPLUT) orientation of MOD17A1 is the best example of this type of externalization, stored in the static ancillary HDFEOS (MOD17_ANC_v21.hdf) file available to the algorithm at runtime. We also store all the defining characteristics of all ESDT product gridfields in this ancillary file, allowing minor file specification changes to be effected from outside the software.

The following diagram illustrates the high level organization (schema) used in MOD17A1, MOD17A2 and MOD17A3:

MODIS PGE 36,37,38
MOD17 Algorithm Component: PSN_NPP
Software Schema

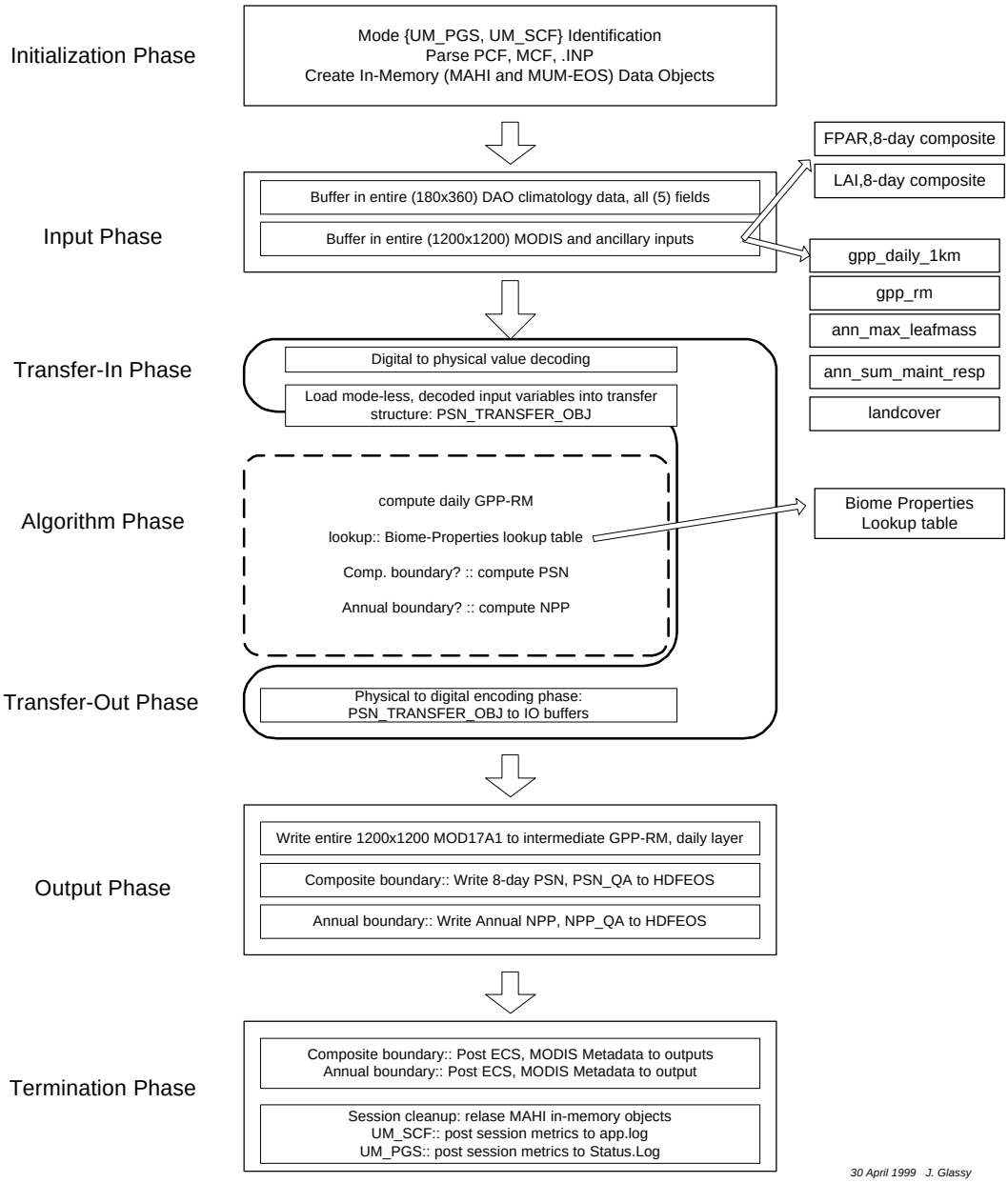

30 April 1999 J. Glassy

5.4 Spatial Map Projection Used

The MOD17A1,A2 and A3 algorithms, like most MODIS Land processes, are organized to accept global coverage inputs, and produce global output coverages either 8-day (PGE-37) or annually (PGE-38) timestep. Rather than process synoptic 1 KM spatial resolution images, the MODIS Land team has adopted a contiguous land tile scheme, based on the Integerized Sinusoidal Grid -- a map projection derived from the sinusoidal map projection (with the General Cartographic Map Projection code of GCTP_ISINUS).

This projection defines a total of 648 tiles globally, at 10 degree resolution. We currently estimate that ***289 tiles of 648*** will be classified as "land" tiles, and thus represent the maximum spatial extent our global algorithms will process. Refer to http://modland.nascom.nasa.gov/developers/bndrytb2.html for additional details. The figure below graphically depicts the IS grid (assuming the standard 10 degrees processing tiles) we expect to work with at-launch. Each individual tiles in this grid includes approximately 1200 x 1200 1 km pixels:

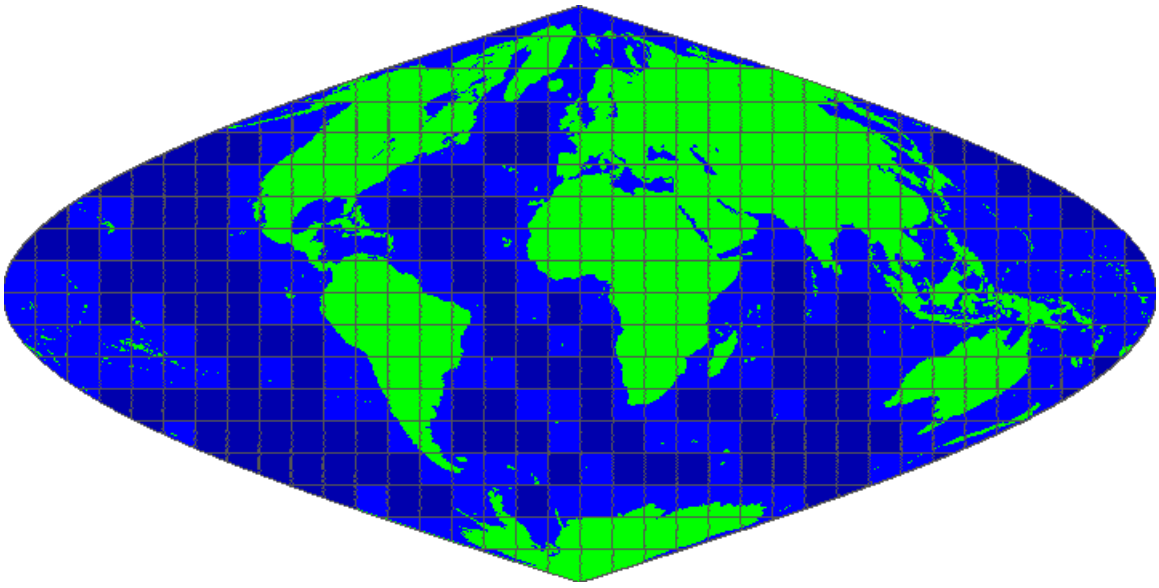

5.5 Data Requirements and Dependencies

The MOD17 PGE software suite (PGE 36,37,38) is positioned at the end of the L3/L4 MODIS Land processing chain; no downstream processes accept MOD17 data products as input. Our algorithms are therefore quite dependent on the quality and correct functioning not just of the MODIS instrument itself, but on the upstream processing as well. The following diagram illustrates the input I/O dependencies for MOD17A1, MOD17A2, and MOD17A3 ESDTs:

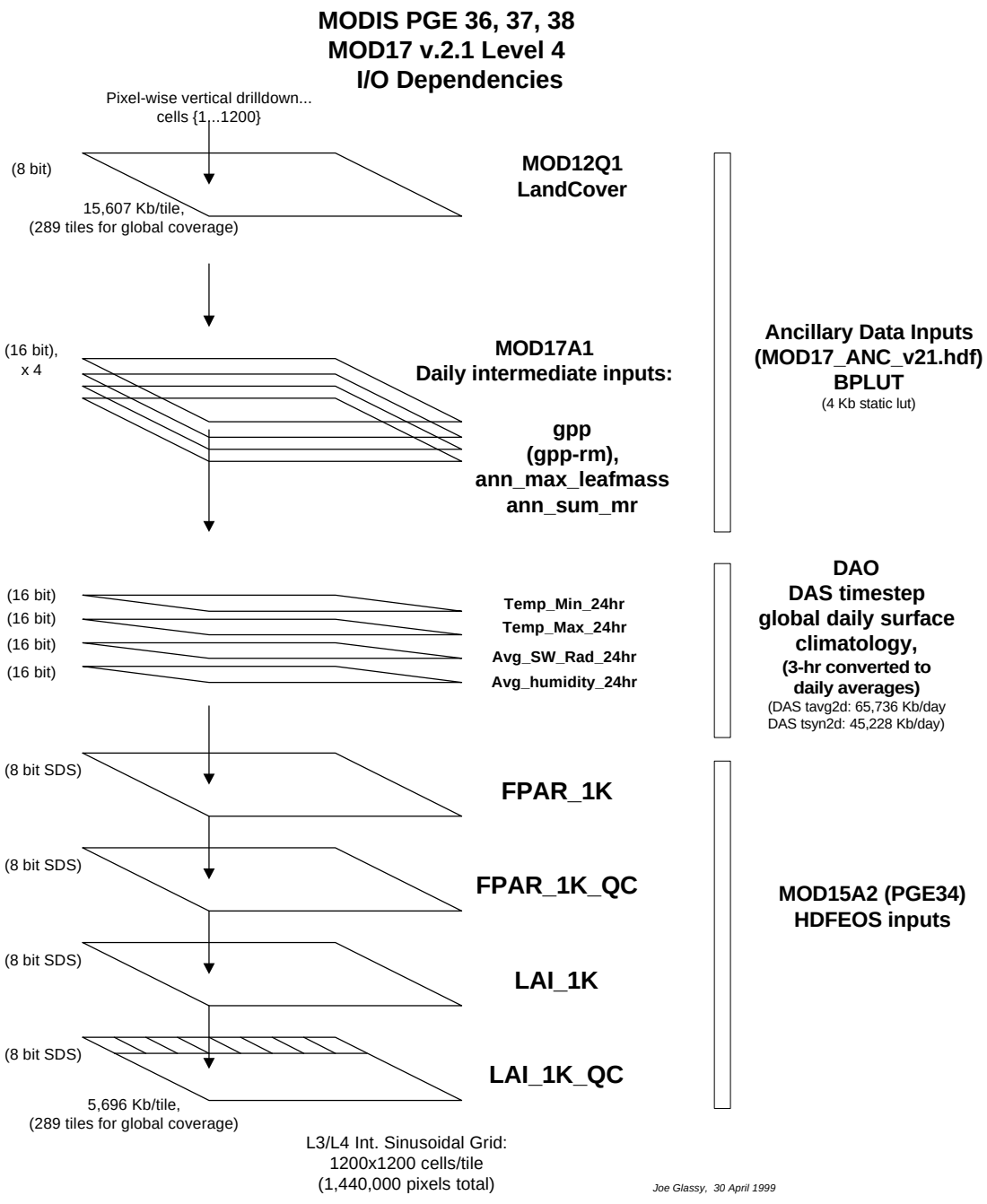
MODIS PGE 36, 37, 38
MOD17 v.2.1 Level 4
I/O Dependencies
Pixel-wise vertical drilldown...
cells {1,..1200}
(8 bit)
15,607 Kb/tile,
(289 tiles for global coverage)
MOD12Q1
LandCover
(16 bit),
x 4
MOD17A1
Daily intermediate inputs:
gpp
(gpp-rm),
ann_max_leafmass
ann_sum_mr
Ancillary Data Inputs
(MOD17_ANC_v21.hdf)
BPLUT
(4 Kb static lut)
(16 bit)
(16 bit)
(16 bit)
(16 bit)
Temp_Min_24hr
Temp_Max_24hr
Avg_SW_Rad_24hr
Avg_humidity_24hr
DAO
DAS timestep
global daily surface
climatology,
(3-hr converted to
daily averages)
(DAS tavg2d: 65,736 Kb/day
DAS tsyn2d: 45,228 Kb/day)
(8 bit SDS)
FPAR_1K
(8 bit SDS)
FPAR_1K_QC
(8 bit SDS)
LAI_1K
(8 bit SDS)
LAI_1K_QC
MOD15A2 (PGE34)
HDFEOS inputs
5,696 Kb/tile,
(289 tiles for global coverage)
L3/L4 Int. Sinusoidal Grid:
1200x1200 cells/tile
(1,440,000 pixels total)
Joe Glassy, 30 April 1999

5.5.1 Data Inputs

The at-launch AM-1 (PGE 36,37,38) PSN, NPP algorithm requires severally spatially defined input datasets, as well as a Biome Properties Lookup Table (BPLUT). All spatial inputs are projected on the MODIS standard land grid, called the Integerized Sinusoidal (IS) grid at 1KM resolution and are stored as NASA HDFEOS files organized using MODIS Land tiling scheme. We understand that this gridded map projection will eventually be adopted into the standard USGS General Cartographic Transform Package (GCTP) suite of map projections, known by the unique GCTP macro, GCTP_ISINUS.

The BPLUT contains one record per MODIS (MOD12Q1) land cover type defined --currently 14. Refer to Table X.XX for a complete description of these types. The BPLUT stores a table of model coefficients which provide the key driving behavior of the internal algorithm. Several of the BPLUT coefficients influence the calculation of the epsilon (PAR conversion efficiency, or light use efficiency) factor. Epsilon is one of the most critical terms in our formulation, since it does not stem from a direct biophysical input. The collective inputs to the PSN, NPP algorithm are divided into several categories:

- MOD17A1 intermediate daily (e.g. cumulative state variables, updated over the year)
- MODIS 8-day FPAR, LAI composite data.
- DAO DAS daily global surface climatology, (pre-launch resolution is 2.0 by 2.5 degree (91x144), with the anticipated at-launch resolution of 1.0 by 1.0 degree resolution, 180x360)
- One static ancillary HDFEOS data table (e.g. MOD17_ANC_v21.hdf), serving as a container for the BPLUT and other static ancillary data.

In the section below, we describe each of the primary PSN, NPP algorithm inputs in more detail.

5.5.2 Intermediate Daily Inputs to PSN, NPP

The intermediate inputs (cumulative updated state variables) are supplied via a daily intermediate state HDFEOS tile file that contains (4) 2 dimensional numeric science data sets (SDSs), as a set of 1200x1200 1KM pixels:

- **Gpp_Daily_1km**. The accumulated daily gross primary productivity term; carbon units
- **Gpp_Rm_1km**. The accumulated daily gross primary productivity, minus maintenance respiration in carbon units.
- **AnnMax_LeafMass_1km**. The annual maximum leaf mass, an estimate of leaf mass for the 1KM pixel.
- **AnnSum_Mr_1km**. The annual sum of maintenance respiration for the 1KM pixel.

5.5.3 MODIS Daily Inputs

The MODIS daily pixel-wise spatial inputs projected on the Integerized Sinusoidal (IS) grid, required by our PSN, NPP algorithm include:

- the most recent 8-day 1 km global fraction of photosynthetically active radiation (FPAR) term, from the MODIS PGE 34 (MOD15A2) 8-day algorithm.

- the most recent 8-day 1 km global leaf area index (LAI) term, from the MODIS PGE 34 (MOD15A1) 8-day algorithm.

- the at-launch MODIS 1km (MOD12Q1) land cover product (14 land cover classes)

- the daily surface global climatology (3-hour timestep) variables from the (2) Data Assimilation Office (DAO) ***GEOS-1 DAS timestep*** climate modeling process using an at-launch spatial resolution of 1 degree by 1 degree geographic resolution on the geographic grid:
  1) DAS assimilated diagnostic surface (tsyn2d) Synthesis dataset variables:
     a) **t10mi**; instantaneous 10 meter air temperature (Kelvins)
     b) **ps**: surface pressure (hPa)
  2) DAS assimilated diagnostic surface (tavg2d) Energy budget dataset variables:
     a) **t10m**; 3-hour 10 meter air temperature (Kelvins)
     b) **radswg**; incident shortwave solar radiation (W/m^2)
     c) **q10m**; specific humidity (g water per Kg air)

- (4) ***daily*** climatology fields, which are internally derived from the above DAS fields daily temperature at runtime by MOD17A1:
  a) average 24 hour daily temperature (deg C)
  b) daily 24 hour minimum temperature (deg C)
  c) actual vapor pressure (derived from DAO specific humidity, in Pa units)
  d) incident shortwave solar radiation (MJ/m2 per 3-hour timestep).

5.5.4 Ancillary Inputs

The main a-spatial ancillary input required by PGE 36/37/38 is the biome properties lookup table (BPLUT). This externally defined table contains one record per land cover (or biome) definition. These coefficients may be updated whenever better quality parameters become available via on going ecosystem research.

The BPLUT for the V.2.1 at-launch algorithm is a simple table with one record for each MOD12Q1 land cover type defined. Each record consists of (16) coefficients used in the daily, 8-day period, and annual ecosystem variable calculations. Refer to Table XX.XXX for the full BPLUT and description.

Table 5.x Biome properties lookup table (BPLUT) Schema		
Field	***Description***	***Units***
Biome	Biome class code {1..14}	N/a
Epsilon_max	Maximum theoretical light use efficiency	kg C/MJ PAR / m^2 /day
Tmin_min	Lowest minimum daily temperature	° C

Tmin_max	Highest minimum daily temperature	° C
VPD_max	Highest daily vapor pressure deficit	Pa
VPD_min	Lowest daily vapor pressure deficit	Pa
SLA	Specific leaf area	leaf area / kg leaf C
Q10_mr	Q10 maintenance respiration factor	Kg C
Froot_leaf_ratio	Fine root leaf ratio	unitless
Livewood_leaf_ratio	Live wood leaf ratio	unitless
Leaf_mr_base	Leaf maintenance respiration base value	Kg C
Froot_mr_base	Fine root maintenance respiration base value	Kg C
Livewood_mr_base	Live wood maintenance respiration base value	Kg C
Leaf_gr_base	Leaf growth base value	Kg C
Froot_leaf_gr_ratio	Fine root to leaf growth ratio	unitless
Livewood_leaf_gr_ratio	Live wood to leaf growth ratio	unitless

5.5.4.1 Climatology Inputs from the DAO

The NASA Data Assimilation Office (DAO) at NASA Goddard Space Flight Center (GSFC) produces a multi-year gridded global atmospheric data set for use in climate and biophysical research. They maintain a series of WWW URL's with a considerable volume of documentation on the many variants of these climatology data products. The following description on the Data Assimilation System (DAS) re-analysis datasets was adapted from information at the DAO URL:

http://dao.gsfc.nasa.gov/experiments/assim54A.html

The DAS datasets are produced using a fixed assimilation system designed to minimize the spin-up in the hydrological cycle. By using a non-varying system, the variability due to algorithm change is eliminated, and geophysical variability can be more confidently isolated. The DAO group plans on producing a DAS 1 degree by 1 degree by 20 level gridded dataset at 6 and 3 hour intervals at launch. Our Montana algorithms use DAS GEOS-1 Multiyear assimilation Re-analysis timeseries dataset variables, packaged in HDFEOS "grid" files such that each 3-hour timestep variable is stored in BSQ format with dimensions [8][181][360]. The two classes of DAS product we use are:

- DAS.flk.asm.tavg2d_eng_x.AM100 (Energy)
- DAS.flk.ams.tsyn2d_mis_x.AM100 (Synthetic)

A sample of the DAO 10 meter temperature field we use is shown below. Notice that the DAO gridding scheme places origin at the southernmost cells, so the visualized images appear upside down:

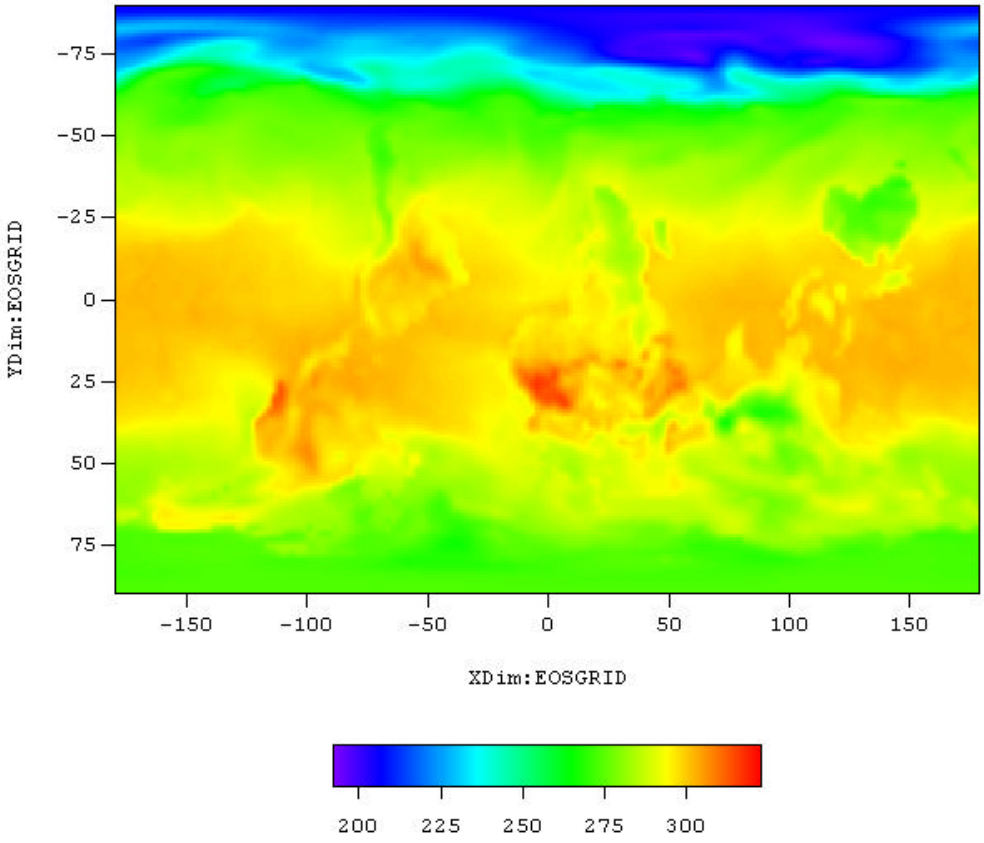

5.6 Compute Loads and Storage Requirements

The at-launch computational metrics for PGE 36,37,38 (MOD17A1,A2,A3) are shown in the table below:

Table 5.4 : PSN, NPP Algorithm Computational Metrics and Storage Loads		
Algorithm/ESDT	MFLOPS	Storage Load (Gb/8-day period)
MOD_PR17A1	17.10	
MOD_PR17A2	17.44	4284 Kb/tile, 0.44 Gb/8-day period
MOD_PR17A3	18.84	4284 Kb/tile, 0.44 Gb/annually
Totals:		

5.6.1 CPU Load Calculation Methods

IS grid tiles are classified as "land" when at least 1 or more 1KM pixel in the 0.50 degree tile region is classified as "land", so we estimate that 289 of the total 648 IS tiles

will be processed as land tiles. Note that only our (8-day PSN) MOD17A2 and (annual NPP) MOD17A3 ESDTs are archived at the DAAC.

For the daily storage load estimate, we assume (a worst case) that all (289) "land" tiles globally are produced daily, and that each archived product tile is (4,386,899 bytes, or 4,284 Kb in size), we have (((4284 Kb/1024)*289 tiles)/1000=1.64 Gb/day.

The methodology used to estimate the MFLOPS is specific to the SGI 64 bit workstation class (using the IRIX 6.4.x operating system), with 2 or more R10000 CPUs running at 195mhz. To obtain the MFLOPS estimate, we built and ran a special form of the algorithm on our SGI Octane (dual R10000,195mhz) workstation using the SGI IRIX "perfex" utility. For our MOD_PR17A1.exe algorithm, we used:

perfex -a -mp -y MOD_PR17A1.exe >& MOD17A1_MFLOPS.report

Note that the MFLOPS value obtained from this utility technically refers to millions of floating point ***instructions*** per second not millions of floating point ***operations*** per second, and due to the fact that there are sometimes multiple instructions per "operation", the value reported is not exact.

5.7 PSN, NPP Algorithm Logic

The PGE 36 (PSN, NPP) algorithm is executed daily on a series of (ca 289) MODIS 1 Km "land" processing tiles. The remainder of the tiles are dominated by ocean, ice, or rock landforms as determined by MODIS land cover classification and the standard MODIS land-sea mask. Each land processing tile represents a land area of approximately 1200 x 1200 1km pixels. The algorithm logic is time sensitive, recognizing and responding to one of the following mutually exclusive (temporally triggered) boundary events:

- …a simple daily update (that ***is not*** coincident with an 8-day composite period or annual period boundary), via ***psn_modis_daynpp()***
- …an 8-day composite period boundary event, via ***psn_calc_science()***
- …an annual period boundary event (immediately followed by an end-of-year reset action), via ***psn_modis_annnpp()***
- …8-day composite period and annual period boundary event coincident to each other.

Note that for each boundary event beyond the first listed above, the ***daily update action is always*** performed first via a separate invocation of MOD_PR17A1. When an 8-day or annual boundary is encountered, the ECS scheduler invokes MOD_PR17A1.exe again in the appropriate mode, keyed from the RUNTIME INPUT .PCF "PSN_PCF_BOUNDARY" flag values as detailed in the production rule summary shown in **Table 5.1** . After each of the above events are encountered, appropriate state and driving variables are updated or reset.

5.7.1 Daily Calculations

The following steps are performed to calculate each day's intermediate gross primary production (PSN), gross primary production minus maintenance respiration (GPP-RM), and net primary productivity (NPP) variables

1. A photosynthetically active radiation (PAR) conversion efficiency (epsilon) is first computed and then attenuated by two controls applied to a maximum value established for each vegetation (biome) type. These controls are:
   a) control due to cold night temperature
   b) control due to daytime vapor pressure deficit

We calculate the daily per-pixel epsilon using:

epsilon = epsilon_max × tmin_scalar × vpd_scalar

where:

epsilon : PAR conversion efficiency,
epsilon_max : maximum theoretical epsilon,
Kg C/ MJ PAR/ m^2/day (where PAR is photosynthetically active radiation)
tmin_scalar : scalar for minimum daily temperature, ° C.
vpd_scalar : scalar for vapor pressure deficit, Pa.

2. The simple daily gross primary productivity for the model day is then calculated as a function of net incident shortwave radiation, FPAR, and epsilon:

gpp = rnet × 0.45 × fpar × epsilon

where:

gpp: gross primary productivity, approx. equiv. to simple PSN
rnet : net incident shortwave radiation, W / m^2 / ha
fpar : fraction of photosynthetically active radiation {0.0 <= fpar <= 1.0}
epsilon : light use efficiency index { 0.0 <= e <= 1.0 }

3. The daily maintenance respiration "costs" are then estimated, using a 20°C base temperature:

leafmass = lai / sla

where:

lai : leaf area index, m^2 leaf / m^2 ground area
sla : specific leaf area; as projected leaf area / Kg leaf C

froot_mass = leafmass × froot_leaf_ratio

where:

froot_mass : fine root mass, Kg
leafmass : leaf mass, Kg
froot_leaf_ratio : ratio of fine root to leaf mass

$$leaf\_mr = leafmass \times leaf\_mr\_base \times q10\_mr^{[tavg-20.0)/10.0]}$$

where:

leaf_mr : leaf maintenance respiration, Kg C
leafmass : leaf mass, Kg C
leaf_mr_base : base leaf mass, Kg C

$froot\_mr = frootmass \times froot\_mr\_base \times q10\_mr^{[tavg-20.0)/10.0]}$

where:

frootmass : fine root mass, Kg C
froot_mr_base : base fine root maintenance respiration, Kg C
q10_mr : maintenance respiration assoc. with Q10

where:

$Mrindex = q10\_mr^{[tavg-20.0)/10.0]}$, daily maintenance respiration index

4. Next we calculate a cumulative daily term for estimating annual net primary productivity (NPP) :

$Npp = gpp - leaf\_mr - froot\_mr$;

where:

Npp : net primary productivity, Kg carbon / hectare
gpp : gross primary productivity, Kg C/ha
leaf_mr : leaf maintenance respiration, Kg C
froot_mr : fine root maintenance respiration, Kg C

5. To incrementally build the annual net primary productivity term, we maintain a series of daily pixel-wise terms, calculating the annual growth (for live wood, leaf, and roots), to appropriately take plant and soil respiration into account. First, live wood maintenance respiration is calculated:

$livewoodmass = ann\_leafmass\_max \times livewood\_leaf\_ratio$

where:

livewoodmass : live wood mass, Kg C.
ann_leafmass_max : annual maximum leaf mass for the given biome, Kg C
livewood_leaf_ratio : ratio of live wood mass to leaf mass

$livewood\_mr = livewoodmass \times livewood\_mr\_base \times annsum\_mrindex$

where:

livewood_mr : live wood maintenance respiration, Kg C
livewoodmass : live wood mass, Kg
livewood_mr_base : live wood maintenance respiration base level, Kg C
annsum_mrindex : the annul summation of the maintenance respiration term: $q10\_mr^{[tavg-20.0)/10.0]}$

Next, annual mandatory growth respiration and maintenance costs are estimated:

leaf_gr = ann_leafmass_max * ann_turnover_proportion * leaf_gr_base

where:

leaf_gr = leaf growth respiration, Kg C
ann_leafmass_max : annual leaf mass maximum, Kg C
ann_turnover_proportion : annual turnover proportion
leaf_gr_base : base leaf growth respiration

froot_gr = leaf_gr $\times$ froot_leaf_gr_ratio

where:

froot_gr : fine root growth respiration costs
froot_leaf_gr_ratio : ratio of fine root growth respiration to leaf growth respiration

livewood_gr = leaf_gr $\times$ livewood_leaf_gr_ratio

where:

livewood_gr : live wood growth respiration
leaf_gr : leaf growth respiration
livewood_leaf_gr_ratio : ratio of livewood to leaf growth respiration

deadwood_gr = leaf_gr * deadwood_leaf_gr_ratio

where:

deadwood_gr :dead wood growth respiration
leaf_gr : leaf growth respiration
deadwood_leaf_gr_ratio : ratio of deadwood growth respiration to leaf growth respiration

Last, we calculate the per-pixel net primary productivity (annual NPP) as the sum of a ***cumulative daily*** NPP accumulated throughout the model year, minus the grow respiration terms calculated from leaf, fine root, livewood and deadwood :

annnpp = annsum_daynpp - livewood_mr -
leaf_gr - froot_gr - livewood_gr - deadwood_gr

where:

annnpp : annual NPP

annsum_daynpp : annual sum of daily NPP
livewood_mr : live wood maintenance respiration
leaf_gr : leaf growth respiration
froot_gr : fine root growth respiration
livewood_gr : live wood growth respiration
deadwood_gr : dead wood growth respiration

5.7.2 Methods for computing the 8-day PSN composite

The NASA MODIS 8-day PSN composite variable is simply the daily "gpp" term described above, as captured on each subsequent 8-day model period boundary. Note that for the 8-day PSN product, respiration is not explicitly accounted for. We acknowledge that our use of the term "compositing" here differs from the more conventional usage, wherein a vertical (pixel-wise) drilldown on series of co-registered data layers is used to form a single pixel wise result value from a candidate set of pixels in the contributing layers. Our compositing procedure is accomplished on the fly via the day to day updating of the intermediate file state fields, so that when a compositing period boundary is encountered, we simply output the latest values (adjusted as needed for respiration) present in the most recent intermediate files.

5.8 Quality Control and Diagnostics

The quality of the PSN and NPP are directly dependent on the quality of the key inputs-- 8-day FPAR, LAI, and daily DAO surface climatology values. In addition, the quality of these outputs is very dependent on the accuracy of the land cover characterization, since so much of the FPAR, LAI, and PSN, NPP algorithm logic is driven from the selection of a "best" land cover classification for the given 1 km pixel. A predominantly "forest" pixel, if misclassified as a "cropland" pixel could potentially lead to very serious model errors in PSN and NPP estimation. From the user's perspective, quality assurance (QA) information stored within the PSN and NPP product files may be divided into two types: tile level QA and pixel level QA. Tile level QA includes standard ECS metadata components (Archive and Core metadata blocks) as well as product specific attributes or PSAs.

The PSAs for PGE 36/37/38 include the following:

Table 5.5 : PGE 36,37,38 (MOD17) PSN, NPP Product Specific Attributes (PSAs)

QA field	***Definition***
QaPctInterpolatedData	percent of pixels interpolated and not computed
QaPctMissingData	percent of pixels missing (not calculated by any means)
QaPctOutOfBoundsData	percent of pixels out of biophysical bounds
QaPctNotProducedCloud	percent of pixels not produced due to cloud related contamination
QaPctNotProducedOther	percent of pixels not produced due to reasons other than cloud problems.
QaPctGoodQuality	percent of pixels (PSN and NPP) rated at "good" or better

	quality.
QaPctOtherQuality	percent of pixels (PSN and NPP) rated at other than "good"
QaPctGoodPsn	percent of PSN pixels rated good or better
QaPctGoodNpp	percent of NPP pixels rated as good or better.
N_days_composited	Number of days composited in this product

5.8.1 Post Production Quality Assurance

The most critical post-production quality ECS metadata fields are the tile level OPERATIONALQUALITYFLAG and OPERATIONALQUALITYFLAG EXPLANATION fields present in each MODIS tile file archived at the Land DAAC. We also intend to set the SCIENCEQUALITYFLAG and associated metadata field, the SCIENCEQUALITYFLAGEXPLANATION. Due to the high frequency of MODIS data production, we currently plan on setting the operational quality flag QA values in just a subset (approximately 10%) of the total tiles produced per unit time.

5.8.2 Pixel level (spatial) QA

A separate, spatially defined 8-bit QA data plane contains additional quality information at the pixel level. These QA "pixels" are bit-packed fields, which means the user must use special methods to extract a range of bits from the 8-bit unsigned character pixel to interpret the values. The LDOPE and SCF QA tools are routinely used perform this extraction. The QA field is internally divided into two basic components; these are the mandatory MODLAND QA bit fields, and the SCF supplied bit fields. The mapping of the 8-bits of the QA pixel is shown below:

Table 5.6 : Spatial QA 8-bit Pixel Organization

QA Field	***Bits***	***Value(s) and Definition***
MODLAND QA used bit	00-00	0=bits 01-02 are set and determined, 1=bits 01-02 are NOT determined.
MODLAND QA bits	00-01	00=atmospherically clear, 01=pixel judged "cloudy" 10=pixel judged "mixed cloud" 11=pixel quality is indicated by another, separate QA field (see bits 06-07 below for our 4-level quality scale).
(Not Used)	02-05	These (4) bits are currently not used
PSN or NPP quality code	06-07	00=best, 01=good, 10=poor, 11=unacceptable

Collectively, these quality control (QC) and assurance fields are provided for two purposes:

- They give the producer a systematic and automated mechanism to routinely assess the quality of the production process in real time. These QC fields thus yield the critical information to facilitate troubleshooting and suggest code corrections when necessary

- they give the end user a method by which to filter various subsets of product data out, against the individual criteria of a their research or applied project.

Automated software tools from the DAAC, LDOPE, and SCF will allow producers (and eventually, end-users) an easy method to extract one or more of these bit subset fields (MODLAND QA bits 0-2, and PSN/NPP quality code (bits 6-7) from the 8 bit quality assurance images.

5.8.3 Assessing Quality of PSN, NPP Products On line

The NASA Land Data Operations Processing Environment (LDOPE), located at Goddard Space Flight Center (GSFC, http://modland.nascom.nasa.gov/QA_WWW/qahome.html) is responsible for first order quality assessment of MODIS Land products. This quality assurance task is shared with the various Science Compute Facilities (SCF) of which the University of Montana (http://forestry.umt.edu/ntsg/projects/modis) is just one. The LDOPE plans to maintain a realtime database populated with a number of quality assessment data fields associated with the MODIS products. The web ordering QA facility will include tools to allow data producers to filter QA data on appropriate selection parameters. Ultimately this is used to accomplish the post-production QA task of setting the OPERATIONALQUALITYFLAG and OPERATIONALQUALITYFLAG EXPLANATION metadata fields, found within the ***CoreMetadata.0*** field in each file). The operational quality flag is by default set to "NOT BEING INVESTIGATED". The SCIENCEQUALITYFLAG metadata field will also be potentially helpful to users interested in the archived data.

5.8.4 System Reliability and Integrity Issues

The compositing scheme we employ requires a set of (289) intermediate daily state files to be maintained (and updated) over the course of an entire model year. As time progresses through the model year, the information in these intermediate files naturally accumulates information for increasingly longer periods. This design increases the risk that during the year, if some of these intermediate files somehow become corrupt or were lost, the re-processing necessary to bring the model state up to the point the state data was lost becomes increasingly burdensome. To assure that such a reprocessing event goes as smoothly as possible, we propose that ECS performs an explicit offline backup of the set of (289) land tiles of daily MOD17A1 intermediate tile files on a periodic basis (e.g. every 8-days if possible, or at least monthly at the least frequent).

In the event that one or more tiles of intermediate data becomes corrupt or missing (e.g. at year-day 230), such a backup scheme will enable re-processing to start at the most recent backup date (say, year-day 222), instead of having to restart at year-day 1 for the current model year. As of Version 2.1 of our PGE 36 MOD17A1 code, a new tile-wise state file-attribute field (int32 **tile_commit_state**[289][366] for tiles 1..289 and year-day 1..366) in the HDFEOS tiles will be added, to independently track which tile/year-day combinations have been successfully "committed". This "tile_commit_state" progress field will allow an automated procedure to quickly

determine how few year-days to "roll-back" the processing clock in the event a re-start becomes necessary.

5.9 Exception Handling

Exception handling for the MOD17A1 (PGE-36,37,38) is performed using the standard ECS compliant SDTPK SMF software layer. In our implementation of this method, we define (4) classes of exceptions according to their severity. A common SMF message file is used for all our algorithms (PGS_MODIS_37150.t/.h). The single letter severity codes {U,W,E,F} were adapted from the SDPTK User's Guide, Section 6.128. The table below summarizes these:

Table 5.7: Univ. Montana SCF Exception Handling (PGE_MODIS_37150.t symbols)

Message Code	***Severity***	***Comments***
MODIS_U_MUM_ADVISORY	Advisory	These messages are used to passively inform the operator or user about a given condition.
MODIS_W_MUM_ADVISORY	Warning	These messages indicate that an out of the ordinary condition has occurred, that may require monitoring further.
MODIS_E_MUM_ADVISORY	Error	These messages indicate that a (non-fatal) program error has occurred which should be investigated as soon as possible.
MODIS_F_MUM_ADVISORY	Fatal exception	These messages indicate that a fatal program error or condition has been encountered. The PGE will halt shortly after performing as much damage-containment as it can.

Generally, when an exception of class MODIS_F_MUM_ADVISORY is encountered, this will necessitate re-running the PGE against the indicated tile, once the cause has been identified and a solution has been determined. A single "collector" exception handling call is made whenever any of these exceptions is encountered. This call routes the text of the message to the (3) standard SDPTK session log files, e.g. (MOD15_StatusLog.log, etc). An example of such a call is shown below:

```
mum_message(MODIS_U_MUM_ADVISORY,
        "lai_main.c","lai_driver","Pixels successfully processed %ld\n",n_total);
```

5.10 Output Products

The MOD15A1 (PGE-33) daily executable produces IS tile (NASA HDFEOS v.2.4 format) output files that are formally identical to the archived 8-day product generated by MOD15A2. The full baselined file format for these may normally be found at:

ftp://modis-xl.nascom.nasa.gov/modisbaselinedcode/COMMON/filespec

To summarize the contents of the archived MOD15A2 FPAR, LAI product file, it contains (4) spatially defined 2D gridfields, the full set of ECS Core, Archive, and Struct metadata fields in Parameter-Value-Language (PVL)/Object Data Language (ODL) format blocks, as well as a small set of gridfield (or SDS) attributes. Note that HDF and HDF-EOS format files use an underlying "xdr" based numeric representation for data, which allows data of any numeric data type to be ported to virtually any compute platform, regardless of the "endian" byte-ordering of the native word on the platform. The common datatype the main gridfields are stored in (e.g. DFNT_UINT8) is a platform independent, unsigned, 8-bit integer type capable of representing numeric values in the range {0 <= dn <= 255} inclusive. The (4) main gridfields are summarized further in the following table:

Table 5.8 : MOD17A2 PSN 8-day and Annual NPP-day archive file summary

Grid Field Name	Datatype	Dimensions	Description
Psn_1km	DFNT_UINT8	1200 x 1200	8-day PSN field
Psn_1km_QC	DFNT_UINT8	1200 x 1200	8-day PSN Quality Control field
Npp_1km_QC	DFNT_UINT8	1200 x 1200	Annual NPP
Npp_1km_QC	DFNT_UINT8	1200 x 1200	Quality control for NPP.

Users may refer to a very complete information base on the ECS metadata concepts may be found at: http://ecsinfo.hitc.com/metadata/metadata.html

Additional ECS information relevant to HDF, HDF-EOS and metadata may be found at:

http://spsosun.gsfc.nasa.gov//InfoArch.html

A set of ECS compliant Product Specific Attributes (PSA) is also included in each tile file, within the CoreMetadata.0 block. These provide users with a very coarse but quick "tile-level" quality assessment for the product file. The table below summarizes these:

Table 5.9 MOD17A2 and MOD7A3 (PGE 37,38) Archive PSAs

PSA Metadata Field Name	Field Description
N_DAYS_COMPOSITED	PGE36 always 1; for PGE37 or PGE38 this is the number of days contributing to the final composite.
QAPERCENTGOODPSN	Percent {0<=p<=100} of PSN pixels rated at

	good (e.g. IsQaMinAcceptQuality) or better
QAPERCENTGOODNPP	Percent {0 <= p <= 100} of NPP pixels rated at good (IsQaMinAcceptQuality) or better.
TILEID	IS Tile ID code, an 8-digit integer that identifies the map projection used, the tile's size code (quarter, half, or full-tile) and the tile's horizontal and vertical position in the grid.

5.10.1 The 8-day PSN composite archive product

The 8-day PSN variable is output globally once per 8 days, projected in the Integerized Sinusoidal (IS) grid, at 1KM resolution. Each IS tile contains 1200x1200 pixels, and is 4,385,858 bytes (for PSN) and 4,385,852 bytes (for NPP) in size. Here is a sample of the MODIS 8-day PSN variable for horizontal tile 12, vertical tile 4, produced using FPAR and LAI values from pre-launch synthetic surface reflectance data:

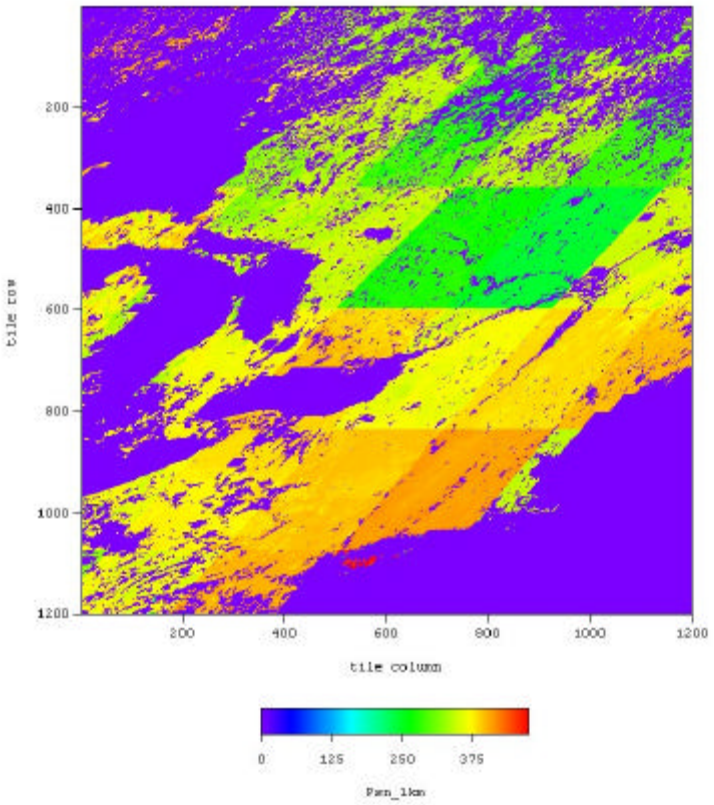

5.10.2 Annual Net Primary Productivity (NPP) archive product

The annual NPP variable is output once annually. Here is a sample of 1 tile of the MODIS NPP output for horizontal tile 12, vertical tile 04 produced using 8-day composited FPAR and LAI values from pre-launch synthetic surface reflectance data. Note that the low values are due to only running the algorithm for a limited number of days for which test data was available:

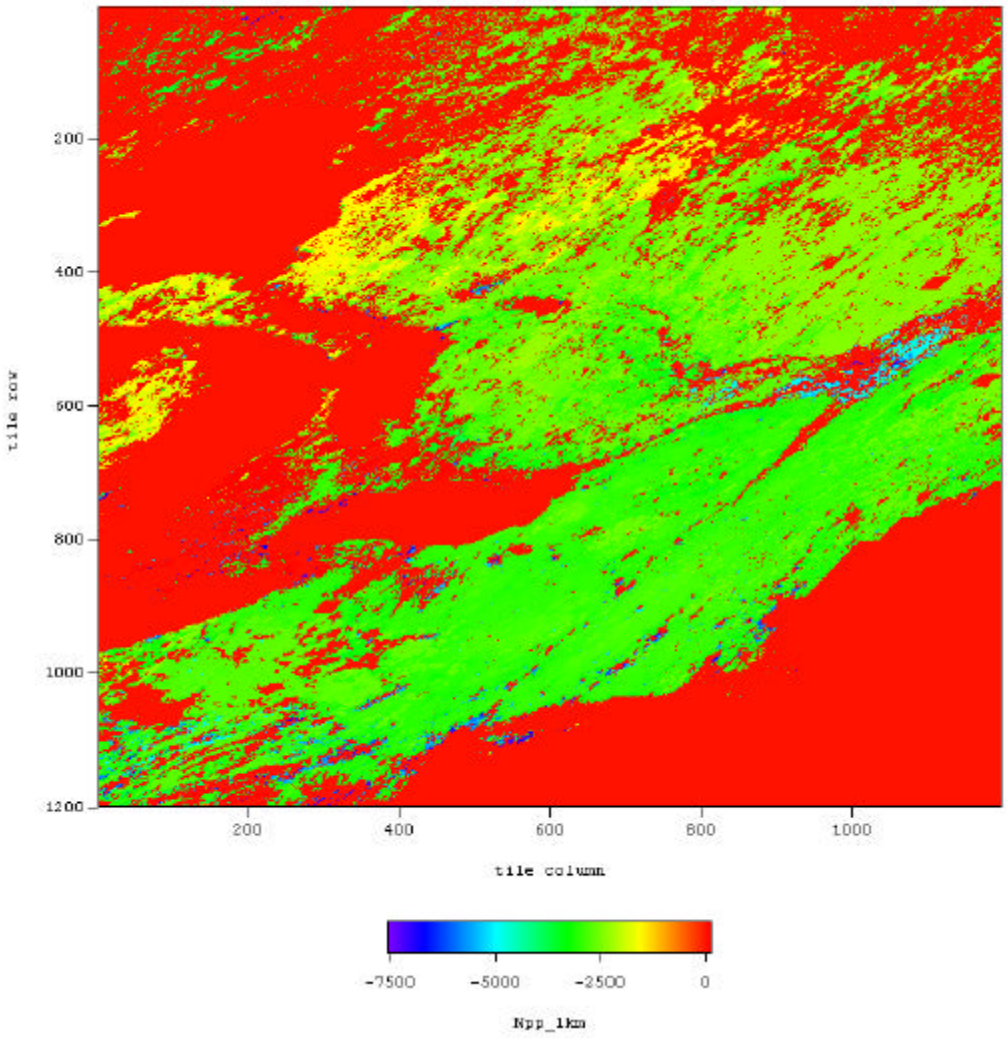

6. VALIDATION PLAN

6.1 Overview of MOD17 (PSN/NPP) validation

Global estimates of biospheric processes will require a permanent network of ground monitoring and model validation points, much like the surface weather station network, to quantify seasonal and interannual dynamics of ecosystem activity, i.e. to

cover the *Time* domain. Remote sensing must be used to quantify the heterogeneity of the biosphere, the *Space* domain. Finally, because these Time and Space measurement regimes cannot provide a complete view of biospheric biogeochemical activity, modeling is required to isolate unmeasured ecosystem processes, and to provide predictive capacity.

6.1.1 Temporal monitoring – carbon, water and energy fluxes

Eddy-covariance flux towers serve as the core infrastructure for three reasons. First, they measure carbon and water fluxes and the surface energy budget, processes directly related to ecosystem function, continuously and semi-automatically, representing an area of approximately 1-3km^2. Second, a global representation of over 80 stations already exists. The current eddy flux network of sites is growing rapidly and becoming increasingly organized. Third, the flux towers provide a critical infrastructure of organized personnel and equipment for other comprehensive measurements, including ecophysiology, structure and biomass of the vegetation, fluxes of other greenhouse gases, and micrometeorology.

Monitoring of the spatial and temporal patterns in the concentration of CO_2, O_2, and their isotopic variants can provide the basis for estimates of carbon cycle fluxes at large scales (Tans et al., 1996). The remarkable achievements from the geochemistry approach, beginning with the observations at Mona Loa which first detected the upward trend in the global atmospheric CO_2 concentration, establish its importance for biospheric monitoring. The limitations in the geochemistry approach for terrestrial monitoring are that it is not spatially-explicit, and generally indicates the net effect of multiple, potentially opposing, processes.

6.1.2 Spatial monitoring - Terrestrial vegetation products from EOS

The field measurements required for this EOS land validation are primarily multi-temporal sequences of vegetation structure and biomass accumulation and turnover, accurately geo-referenced to provide spatial fractions of vegetation structure across the landscape. LAI and NPP, the most directly measured vegetation structural and functional variables, respectively, range by two orders of magnitude among the diverse terrestrial biomes and change seasonally with annual plant growth cycles. Spectral vegetation indices such as the well known NDVI and FPAR are radiometric products that can only be measured instantaneously but can be inferred by vegetation structural measurements, most commonly by LAI. The plans discussed below will measure LAI to provide inferred validation of VI and FPAR, and will measure fractional vegetation cover of regional study areas. Further details can be found at: http://www-osdis.ornl.gov/eos_land_val/valid.html

6.1.3 System processes and integration – ecological modeling

The eddy fluxes and ecophysiological measurements provide process level understanding of ecosystem function that can be incorporated into ecosystem models. However, there will never be sufficient eddy flux towers or field measures to adequately characterize all terrestrial ecosystems under all conditions. Models must then be used to interpolate and extrapolate flux measurements in time and space. Hence, models are and will be a key tool for making regional and global assessments (Waring and Running,

1998). Mechanistic ecosystem models also have the potential for *predicting* how ecosystems will respond to future changes in atmospheric CO_2, temperature, land use change, nitrogen loading and precipitation. The tower fluxes represent a footprint of roughly 1-3 km^2, while NPP is typically measured on ≈ 0.1 ha plot. Process-based terrestrial ecosystem models, driven by spatially represented climate and satellite derived vegetation parameters, are essential for integrating the suite of field-based measurements of inconsistent temporal and spatial scale to provide a complete and consistent view of global biospheric function.

6.2 Global flux tower network (FLUXNET)

The cornerstone of this validation effort is the tower flux network, FLUXNET. This global array of tower sites is currently comprised of regional networks in Europe (EUROFLUX), North America (AmeriFlux), Asia (JapanNet, OzFlux) and Latin America (LBA). Togther, they provide a reasonable coverage of global terrestrial ecosystems (Table 1). The towers provide a continuous and representative measure of terrestrial carbon cycle dynamics, and an important ancillary suite of measurements of energy and water fluxes for interpreting carbon fluxes (**Figure 6.1**).

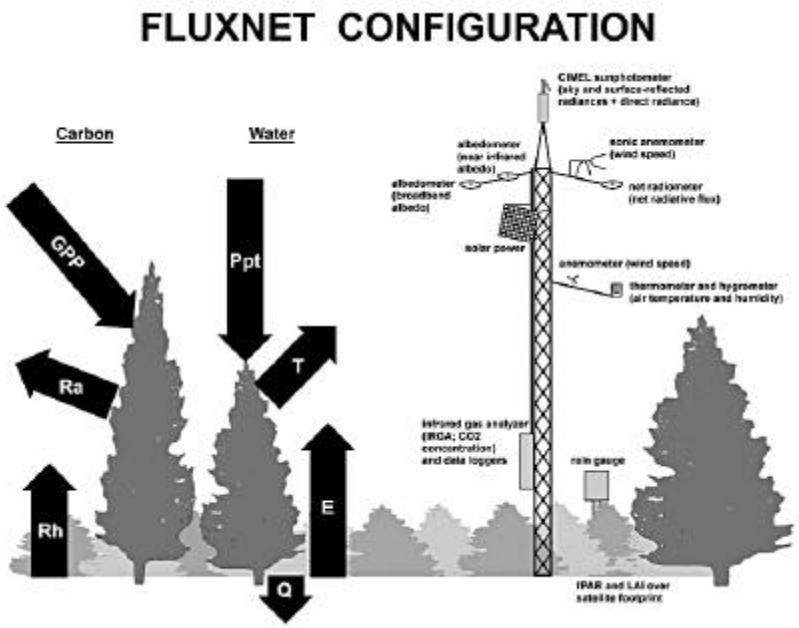

Figure 6.1. A generalized FLUXNET tower configuration diagram, showing instrument deployment and key carbon and water fluxes measured. Atmospheric optical measurements, automated surface spectral measurements, physiological process studies, flask sampling and stable isotope sampling are all additions that can be accommodated into this framework to provide a more versatile monitoring system.

The role of FLUXNET includes coordinating the regional networks so information can be attained at a global scale, ensuring site to site inter-comparability, coordinating enhancements to current network plans and operation of a global archive and distribution center at the Oak Ridge DAAC. The FLUXNET project web address is http://daacl.ESD.ORNL.Gov/FLUXNET/. The web sites contain measurement protocols for consistency, and data on site, vegetation, climate and soil characteristics. It provides

a route for users to gain access of hourly meteorological and flux measurements and proper documentation.

The FLUXNET concept originated at a workshop on 'Strategies for Long Term Studies of CO_2 and Water Vapor Fluxes over Terrestrial Ecosystems' held in March, 1995 in La Thuile, Italy (Baldocchi et al., 1996). The first organized flux tower network was EUROFLUX, which now involves long-term flux measurements of carbon dioxide and water vapor over 15 forest sites in the United Kingdom, France, Italy, Belgium, Germany, Sweden, Finland, Denmark, The Netherlands and Iceland. A website is at: http://www.unitus.it/eflux/euro.html. In 1996, AmeriFlux was formed under the aegis of the DOE, NIGEC program, with additional support by NASA, and NOAA. The website is at: http://www.esd.ornl.gov/programs/NIGEC.

6.2.1 Eddy covariance principles

The eddy covariance method is a well developed method for measuring trace gas flux densities between the biosphere and atmosphere (Baldocchi et al., 1988; Lenschow, 1995; Moncrieff et al., 1996). This method is derived from the conservation of mass and is most applicable for steady-state conditions over flat terrain with an extended tract of uniform vegetation. If these conditions are met, eddy covariance measurements made from a tower can be considered to be within the constant flux layer, and flux density measured several meters over the vegetation canopy is equal to the net amount of material entering and leaving the vegetation. Vertical flux densities of CO_2 and water vapor between the biosphere and the atmosphere are proportional to the mean covariance between vertical velocity and scalar fluctuations. This dependency requires the implementation of sensitive, accurate and fast responding anemometry, hygrometery, thermometry and infrared spectrometry to measure the vertical and horizontal wind velocity, humidity, temperature and CO_2 concentration.

Errors arise from atmospheric, surface and instrumental origins, and they may be random, fully systematic and/or selective (Goulden et al., 1996). Most random errors are associated with violations of atmospheric stationarity and the consequences of intermittent turbulence. Instrument errors are systematic, caused by insufficient time response of a sensor, the spatial separation between a sensor and an anemometer, digital filtering of the time signal, aerodynamic flow distortion, calibration drift, loss of frequency via sampling over a finite space, and sensor noise (Moore, 1986; Moncrieff et al., 1996). The AmeriFlux, Euroflux and FLUXNET programs are attempting to identify and minimize instrumental errors by circulating a set of reference instruments, to which all sites can be compared. Daily-averaged fluxes reduce the sampling errors associated with fluxes measured over 30 to 60 minutes intervals. Hence, daily integrals of net carbon flux can be accepted with a reasonable degree of confidence. Goulden et al. (1996) conclude that the long term precision of eddy covariance flux measurements is +/- 5-10% and the confidence interval about an annual estimate of net canopy CO_2 exchange is +/- 30 g C m^{-2} y^{-1}.

6.2.2 Implementation and Operation

A typical cost for purchasing instruments to make core measurements is on the order of $40 to $50k (US); this cost can double if spare sensors, data telemetry and data archiving hardware are purchased. The cost of site infrastructure is extra and will vary

according to the remoteness of the site (the need for a road and line-power), the height of the vegetation (whether or not a tall tower must be built), and the existence of other facilities. Recent advances in remote power generation and storage minimize the need and cost of bringing line power to a remote site. Advances in cellular telephone technology also allow access and query of a remote field station from home or the office. The requirement for on-site personnel is diminishing, as flux systems become more reliable and automated. At minimum, a team of two individuals are required to operate a flux system, and handle the day-to-day chores of calibration, instrument and computer maintenance, data archiving and periodic site characterization (e.g. soil moisture and leaf area measurements).

Sites in an organized global flux network can also expect to attract additional activities. A synergism between flux and meteorological measurements and an array of other terrestrial science projects is likely. Terrestrial bioclimatology, remote sensing, atmospheric optical characterization, water resource and nutritional biogeochemistry studies are examples of science that are being attracted to the flux network sites.

6.3 Validation of EOS terrestrial vegetation products

6.3.1 Vegetation measurements in the EOS/MODIS grid

EOS will produce regular global vegetation products primarily from the MODIS sensor (Moderate Resolution Imaging Spectroradiometer (Running et al., 1994; Justice et al., 1998). MODIS satellite products will be in a regular grid of square, 1 km^2 cells that do not exactly overlay a tower "footprint." The tower footprints vary in size (up to several km^2), shape, and orientation, depending on location, height above canopy, windspeed, and direction (Hollinger et al., 1994; Waring et al., 1995). In order to permit comparisons of tower-based NEE estimates and the satellite-based NPP estimates from the MODIS grid, certain transformations are needed (**Figure 6.2**). A SVAT model that resolves component carbon balance processes, and validated by local flux tower measurements over a grid of 10-100 km^2 around the tower, provides this scale transformation.

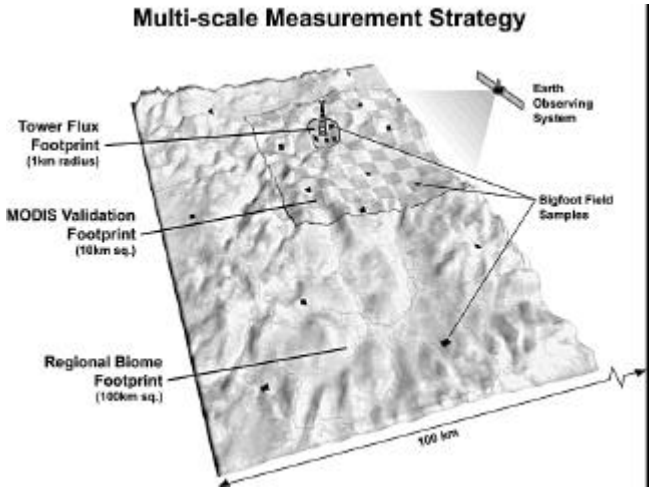

Figure 6.2 Illustration of the three spatial scales that must be considered for ecological scaling and validation. Measures of vegetation parameters (see Table 2) in the atmospheric footprint of the FLUXNET towers are required for SVAT models to simulate the NEE measured by the towers. Second, a larger area of minimum 3x3 km must be sampled to provide ground truth of MODIS LAI and NPP vegetation products. Third, the representativeness of the FLUXNET tower and MODIS sampling site to the larger biome/climate complex must be evaluated by cross biome sampling. Aircraft flux transects and atmospheric flask measurements can provide independent validation of regional flux calculations. Only after all of these scales of measurement are co-validated can comprehensive synthesis of ground data, ecosystem models and satellite data be accomplished.

The most direct measurement of NPP for validation involves harvesting and weighing biomass production in a time sequence. The plot size here is considerably smaller than a tower footprint, e.g. 1 m^2 for clipping in a grassland or 1 ha plots for tree coring and litterfall traps in forests. Multiple NPP measurements made in the 100 km^2 area surrounding a tower serves to extend the model validation over the local environmental gradients and variation in land use.

6.3.2 Quantifying Land surface heterogeneity for EOS validation - BigFoot

Over a site consisting of homogenous vegetation cover and small environmental gradients, the scale inconsistencies between EOS/MODIS NPP estimates and ground-based validation measurements may be minimal. However, many important ecosystems are fairly complex in structure and topography, even over the relatively small area represented by a MODIS cell or a tower footprint. For example, much of the U.S. Pacific Northwest region is characterized by patches associated with forest clearcuts that are generally much smaller than 1 km on a side (Cohen et al., 1998). In the Lake States the choice of grain size up to 1 km greatly affects estimates of land surface occupied by aquatic versus terrestrial systems (Benson and MacKenzie, 1995). The tendency for the scale of human influence on ecosystem carbon flux to fall below the 1 km resolution was recognized during the design phase of the MODIS instrument (Townshend and Justice, 1988), and accounted in part for including channels at 250 m and 500 m in the visible and near-IR wavelengths.

The BigFoot project makes the link between purely satellite-based C flux estimates, tower fluxes and direct field measurements. The BigFoot website is at: http://www.fsl.orst.edu/larse/bigfoot/ . The goal is to develop three fine-grained surfaces (25km^2) using a combination of Landsat Enhanced Thematic Mapper (ETM+), SVAT models, and field observations. These surfaces include the standard EOS products of land cover class, leaf area index (LAI), and NPP. BigFoot currently consists of a set of four sites (all are FLUXNET sites) spanning the climatic gradient from boreal to warm temperate, encompassing several important biomes, and including a variety of land-use patterns. Additional sites will be added in the future, with highest priority being tropical forests, deserts and arctic tundra, and this protocol is being adopted by the GTOS-NPP project globally.

Land cover is an important variable for the purposes of the BigFoot scaling effort because physiological characteristics that influence carbon, nitrogen, and water vapor exchange between terrestrial ecosystems and the atmosphere differ among vegetation cover types (Landsberg and Gower, 1997). In addition, Thematic Mapper-based classifications are often able to resolve specific stages in local successional sequences (e.g. Cohen et al., 1995) and thus may indicate information about levels of coarse woody

debris, an important input to SVAT models simulating heterotrophic respiration. Thus, SVAT models use land-cover type as a stratification factor. Most importantly, these maps will consist of site-specific cover classes that are locally meaningful for ecological function and model parameterization.

LAI has also proved valuable in scaling efforts, and is an input to most existing SVAT models. LAI surfaces will be based on ETM+ imagery combined with field sampling. Following development of land cover and LAI surfaces, NPP grids will be developed for each BigFoot site using SVAT models. These grids will be developed using the models in 2-dimensional mode in conjunction with the site-specific driver surfaces, land cover and LAI, and spatially-distributed climatic drivers based on extrapolations from flux tower meteorological observations. Beside the daily time step validation of GPP and ET at BigFoot sites with flux towers, the BigFoot NPP surfaces will be carefully evaluated for error by reference to a gridded network of ground measurements of NPP. Assuming the errors in these NPP surfaces are acceptable, the fine-grained gridded surface over a 25 km^2 area can then be directly compared to NPP estimates derived from MODIS data over the same area. If the MODIS-based estimates do not satisfactorily agree with the BigFoot estimates, it will be critical to identify causal factors.

BigFoot will isolate and test three key factors -- spatial resolution, land cover classification scheme, and light use efficiency factors -- that may contribute to differences between EOS-based and BigFoot NPP estimates. To evaluate the role of spatial resolution, the BigFoot 25 m grids for input variables will be aggregated to resolutions of 250 m, 500 m, and 1000 m using a variety of standard and experimental algorithms. Model runs will then be made at each spatial resolution and comparisons of simulated NPP at the different resolutions (including 25 m) will be made with each other and with the EOS/MODIS 1 km NPP products. Results of these scaling exercises over the range of biomes and land use patterns included in BigFoot will test both SVAT models and satellite-based NPP algorithms.

6.4 System integration and scaling with models

To transform basic tower flux and flask data and global remote sensing into an effective validation program, three steps are now required. *First*, SVAT models must be used at each tower site to compute the important system processes that cannot be directly measured, such as the component carbon fluxes of NEE. In order to operate the SVAT model, certain key site and vegetation characteristics must be measured to parameterize the model for the tower area (**Table 2**). *Second* to provide a spatial frame of reference for the tower site, satellite derived characterization of the surrounding vegetation is needed. The EOS/MODIS standard spatial resolution is 1 km, so to provide adequate sample size, approximately a 10x10 km area needs to be efficiently sampled. *Third*, with validated MODIS vegetation products of landcover, LAI and NPP, a larger region can now be evaluated to understand how the flux tower data represents the broader biome and region. This three step scaling process, evaluating the tower footprint of ≈1 km^2, then the EOS/MODIS footprint of ≈100 km^2, and finally the regional biome footprint of thousands of square kilometers provide the scaling logic for global monitoring (**Figure 6.2**).

6.4.1 SVAT model requirements for 1-d flux modeling

SVAT models have been designed with a wide array of system complexities (**Figure 6.3**). For example, some models define each age class and branch whorl of leaves, while others use only simple LAI. Time resolutions of various models range from 1 hour to monthly. The land surface models such as BATS and SiB in GCMs are effectively SVAT models despite being used at very coarse spatial grids (Dickinson, 1995). SVAT models of highest relevance to FLUXNET have time resolutions in the hourly-daily domain, treat canopy structure fairly explicitly, and resolve components of the carbon balance (photosynthesis, heterotrophic and autotrophic respiration and allocation). Likewise, stand water balance components, (canopy interception, snowpack, soil water storage, evaporation and transpiration) must be explicitly computed. All of the leading SVAT models incorporate some treatment of nutrient biogeochemistry interactions with carbon and water processes. However, given these requirements, there are still many available and appropriate SVAT models (see recent books by Landsberg and Gower, 1997; Waring and Running, 1998). What is needed for a coordinated global program are some common protocols, of variables, units, timesteps, etc. that would allow cooperation and intercomparisons amongst groups using different SVAT models in their space/time scaling. The 1-d SVAT models require meteorological driving variables measured at the tower, the initializing biomass components of the vegetation, and certain soil physical and chemical properties. All SVAT models have somewhat different specific requirements, but the general list of inputs found in Table 2 covers most of them.

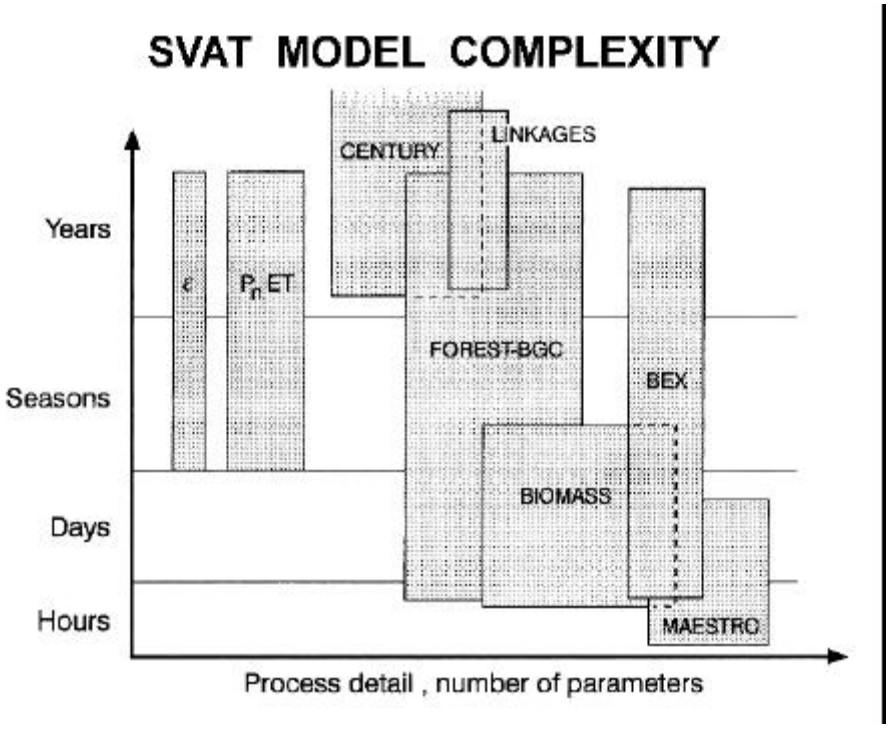

Figure 6.3. A general evaluation of the varying time scales and mechanistic complexity inherent in various current Soil-Vegetation-Atmosphere-Transfer (SVAT) models. The MODIS global NPP estimate is represented by the ε, a model of minimum process complexity. Models of higher process detail are

required to validate and interpret the ε models, but cannot be run globally because of lack of data and computing limitations (redrawn from Landsberg and Gower, 1997).

6.4.2 Relating NEE and NPP in the flux tower footprint

Flux towers measure the net gain or loss of carbon over hourly to daily time scales (Fan et al., 1995; Baldocchi et al., 1996; Frolking et al., 1996; Goulden et al., 1996). Because SVAT models estimate photosynthesis, autotrophic and heterotrophic respiration separately, they generate separate estimates of NEE and NPP. Besides comparisons of measured and modeled NEE and NPP, one specific output of these models is daily GPP (gross primary production or net photosynthesis). This modeled GPP can be compared directly to an estimate of GPP derived from tower data (daytime NEE minus estimated daytime ecosystem respiration) (**Figure 6.4**). Once a SVAT model is parameterized and validated over a daily time step at a tower site, it can be run to simulate NPP for a full year. Using direct field measurements of NPP made at the tower sites, model estimates of annual NPP can also be validated. The SVAT models thus provide an essential link between NEE measurements by the tower, and NPP, the C-flux

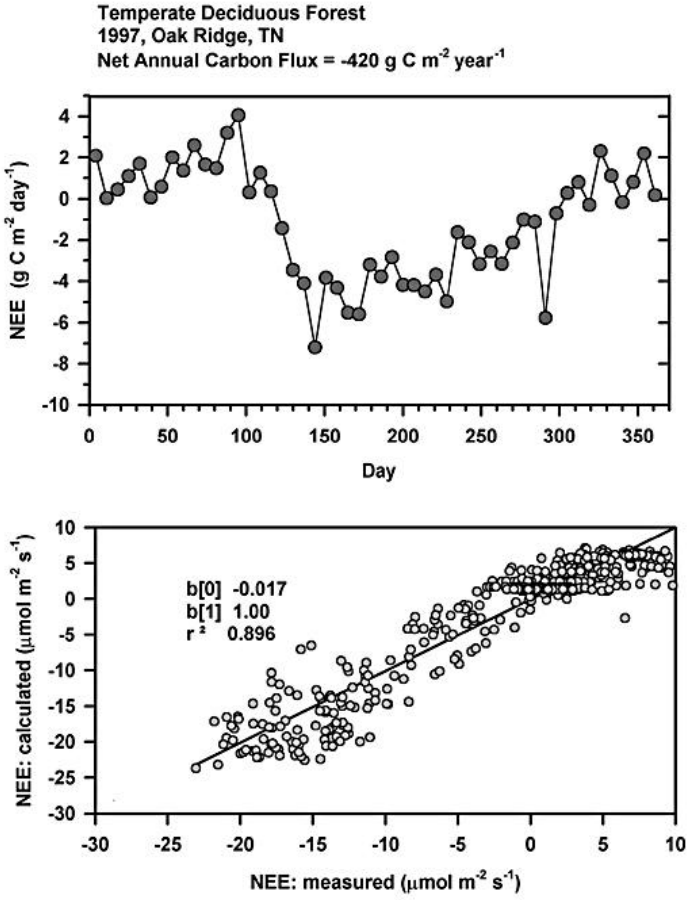

variable most relevant to the standard EOS NPP product.

Figure 6.4a. An example of FLUXNET carbon balance data, weekly net ecosystem exchange (NEE) for 1997 measured by an eddy covariance fluxtower for a temperate deciduous forest, and, **6.4b**. The comparison of SVAT model simulation of NEE to observed NEE in 7a (Baldocchi, unpublished).

6.4.3 Biospheric model intercomparisons

Another approach to assess accuracy of biospheric models when direct measurements are not possible is by global model intercomparisons. Major discrepancies in results amongst models draw attention to potential problem areas and datasets or weak process understanding. Two international biospheric model intercomparison activities are currently underway.

The ongoing IGBP sponsored 1995 Potsdam (PIK)-NPP model intercomparison can use FLUXNET derived NPP estimates to test global NPP model estimates at locations sampled by the network. The website is at: http://gaim.unh.edu/ . The 1995 Potsdam NPP model intercomparison project was an international collaboration that produced single-year global NPP simulations (Cramer et al., 1999). There were large discrepancies amongst models of NPP in northern boreal forests and seasonally dry tropics. Over much of the global land surface, water availability most strongly influenced estimates of NPP, however, the interaction of water with other multiple limiting resources influenced simulated NPP in a non-predictable fashion (Churkina and Running, 1998).

VEMAP http://www.cgd.ucar.edu:80/vemap/ is an ongoing multi-institutional, international effort addressing the response of terrestrial biogeography and biogeochemistry to environmental variability in climate and other drivers in both space and time domains. The objectives of VEMAP are the intercomparison of biogeochemistry models and vegetation distribution models (biogeography models) and determination of their sensitivity to changing climate, elevated atmospheric carbon dioxide concentrations, and other sources of altered forcing. The completed Phase 1 of the project was structured as a sensitivity analysis, with factorial combinations of climate (current and projected under doubled CO_2),atmospheric CO_2, and mapped and model-generated vegetation distributions. Maps of climate, climate change scenarios, soil properties, and potential natural vegetation were prepared as common boundary conditions and driving variables for the models (Kittel et al., 1995). As a consequence, differences in model results arose only from differences among model algorithms and their implementation rather than from differences in inputs (VEMAP Members, 1995). VEMAP is currently in the second phase of model intercomparison and analysis. The objectives of Phase 2 are to compare time-dependent ecological responses of biogeochemical and coupled biogeochemical-biogeographical models to historical and projected transient forcings across the conterminous U.S. Because the VEMAP project has no validation component, interaction with FLUXNET and EOS can provide direct model validations (Schimel et al., 1997).

6.5 International coordination and implementation

Global validation and monitoring cannot be done without international cooperation that transcends any national agency (**Figure 6.5**).

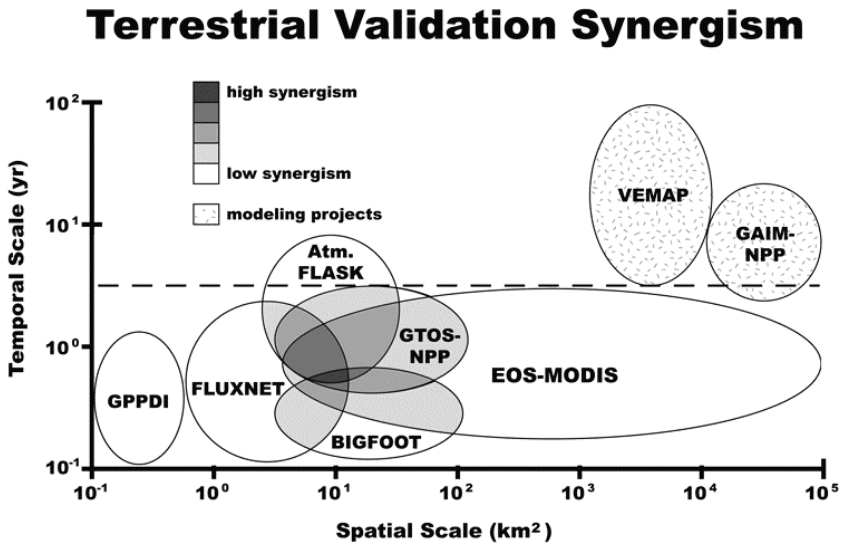

Figure 6.5. Potential synergism of international programs for validating terrestrial ecosystem variables at different space/time scales. Sites contributing to multiple programs have the highest synergism and efficiency. The programs depicted are: GPPDI = Global Primary Production Data Initiative, FLUXNET = the global network of eddy covariance flux towers, Atm FLASK = The global network of atmospheric flask sampling of NOAA/CMDL and C.D. Keeling and others, GTOS-NPP = a special project of the Global Terrestrial Observing System to measure Net Primary Production of field sites worldwide, BigFoot = a study to establish scaling principles for sampling vegetation over large areas, EOS-MODIS = the Moderate Resolution Imaging Spectroradiometer on the Earth Observing System, the primary terrestrial observation sensor, VEMAP = the Vegetation/Ecosystem Modeling and Analysis Project, GAIM-NPP = the International Geosphere-Biosphere project in Global Analysis Integration and Modeling study of global NPP. See text for details of these projects.

When planning global networks, it is essential to recognize that not all facilities have equal levels of scientific activity, however all are needed to provide adequate global sampling. The Global Terrestrial Observing System (GTOS) and terrestrial components of the Global Climate Observing System GCOS have led in designing consistent international measurements for validation and monitoring work (Global Climate Observing System, 1997). The strategy for implementing the plan is being developed in conjunction with the World Meteorological Organization (WMO), and the International Geosphere-Biosphere Programme (IGBP). The plan will provide the necessary climate requirements for GTOS and the terrestrial requirements for GCOS. See http://www.wmo.ch/web/gcos/gcoshome.html

Two core projects of IGBP have been instrumental in developing coordinated terrestrial systems. BAHC is the original project to suggest FLUXNET, and GCTE has led in designing the IGBP Terrestrial Transects. Both GAIM and IGAC now are supporting the continuing development of a global validation and monitoring system. Two internationally coordinated activities appear ready to implement FLUXNET and biospheric monitoring activities, the IGBP Transects, and the GTOS-NPP project.

The IGBP Terrestrial Transects, website at: http://gcte.org/LEMA-IGBP/LEMA-IGBP.html are a set of integrated global change projects consisting of distributed observational studies and manipulative experiments, coupled with modeling and synthesis activities organized along existing gradients of underlying global change parameters, such as temperature, precipitation and land use. The IGBP Terrestrial Transects consist of a set of study sites arranged along an underlying climatic gradient; of order 1000 km in length and wide enough to encompass the dimensions of remote sensing images. The initial set of IGBP Terrestrial Transects are located in four key regions, with three or four existing, planned or proposed transects contributing to the set in each region.

The GTOS-NPP project, (website at http://www.fao.org/GTOS/Home.htm) is being coordinated through the international U.S. Long Term Ecological Network (LTER) office, http://lternet.edu/ilter/ . The goal of the GTOS-NPP project is to distribute the 1km EOS NPP and LAI products every eight days to regional networks for evaluation, and after validation, translation of these standard products to regionally specific crop, range and forest yield maps for land management applications. The project will also provide global validation points for land paramaterization in climate and carbon cycle models.

6.6 Testing MODIS PSN/NPP products in near real-time

Here we describe specific plans for testing and validating MODIS PSN/NPP products on an operational basis using FLUXNET data. We believe only FLUXNET data can provide a continuous, week-to-week validation of the PSN/NPP products. Currently, there are about 80 flux towers globally, spanning various climate-vegetation combinations. Twenty eight of these flux towers are operating in the U.S (Figure 6.6).

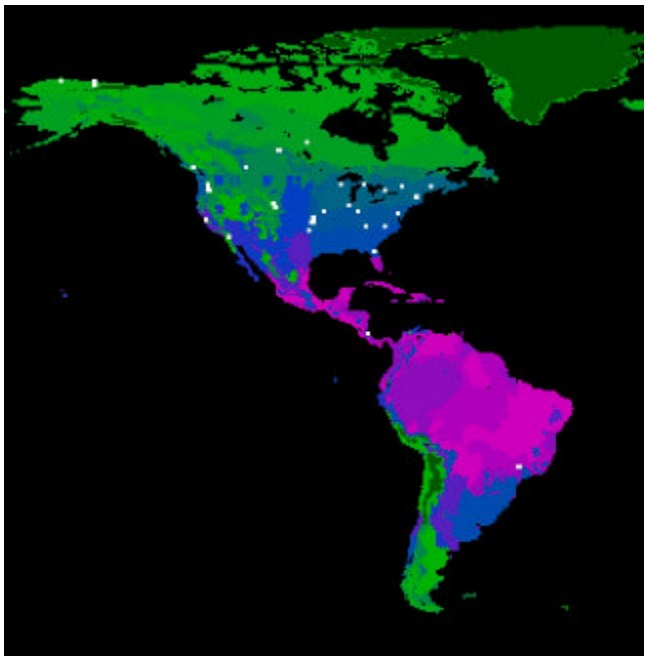

Figure 6.6: Locations of flux tower sites in the U.S. Brief descriptions for each of the 28 sites are given in Table 3.

Our initial plan is to use the 28 sites in our validation scheme; upon successful implementation of the validation protocols we can extend the program to cover all global flux tower sites willing to share their information.

Every 8 days, we will extract MODIS derived NPP product for a 2x2km grid over each of the 28 flux sites in the U.S. This data will be sent automatically to the scientists responsible for each flux tower site.

In return, we obtain micro-meteorological observations (incident solar radiation, air temperatures, humidity and rainfall) over the 8 day period from the flux tower sites. This data will be used first, to test the accuracy of the climate observations (DAO) used in the MOD17 algorithm. Specifically, we would like to test the daily incident solar radiation, air temperatures and humidity. Second, we will replace the DAO climate with observed micro-meteorological data in the MOD17 algorithm and re-compute the NPP. Differences between the two estimates allow us to compute the errors propagated by using DAO climatology. Third, we will use BIOME-BGC calibrated for each flux site to compute various CO2 fluxes on a daily basis, using the observed micro-meteorological data and site specific soil and plant characteristics. BIOME-BGC estimated fluxes would be directly comparable with flux tower estimates (Figure 6.7).

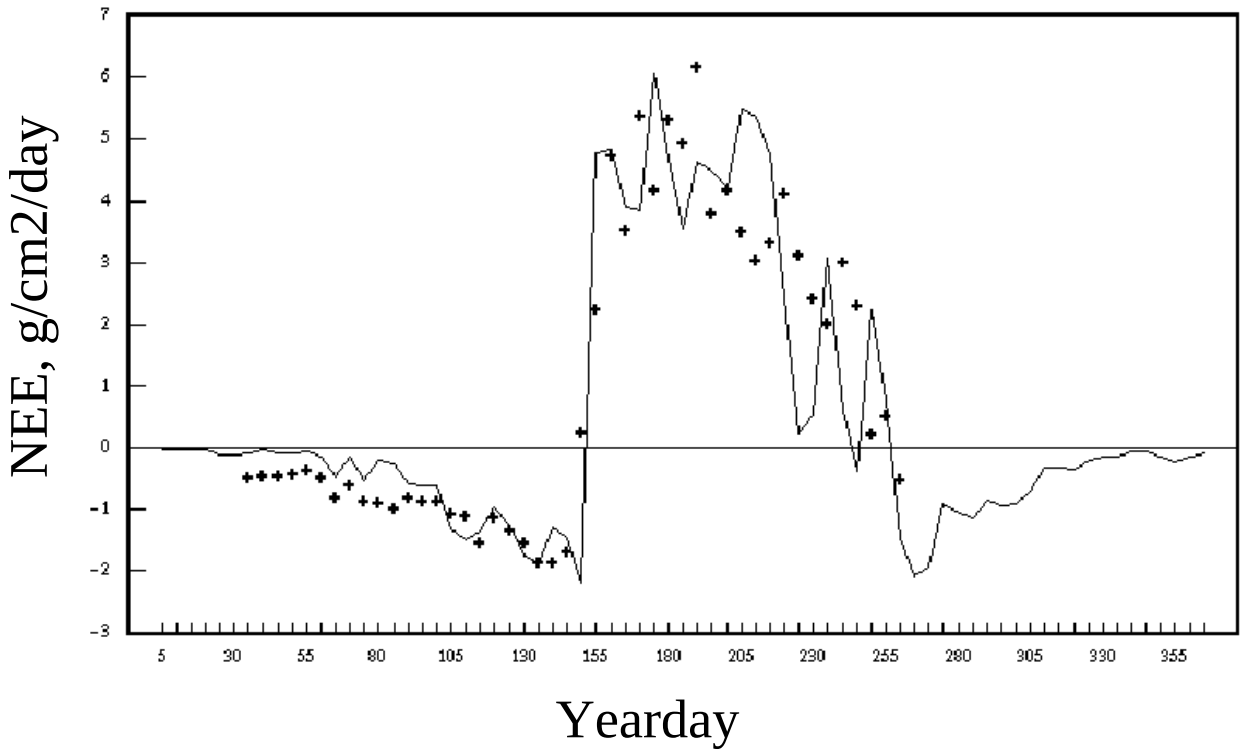

Figure 6.7 : Observed (symbols) and BGC estimated (line) net ecosystem production at BOREAS, showing the ability of BGC to represent seasonal variations in carbon exchange.

Along with testing the carbon fluxes, this scheme also allows seasonal comparison of leaf area index, vegetation phenology, and snow cover derived from

MODIS data with observations collected at the flux sites. Initial efforts will focus on the ability of MOD17 product to characterize the geographic distribution of NPP over the U.S, then the seasonality (start of growing season, mid-summer drought effects on NPP) and finally the magnitudes of carbon fluxes at each site.

Once the scientists responsible for each flux tower site release their flux data, all four products (measured fluxes, BGC simulated fluxes, MODIS-Micromet, MODIS-DAO) will be archived at OAKRIDGE DAAC. With this scheme, a two way cooperation is required between MODIS and FLUXNET scientists. Protocols for data exchange need to be worked out with each flux site, along with a written commitment to participate in this validation program.

Table 6.1 Current biome distribution of the 80 established FLUXNET sites.

Functional Type	Percent
Temperate Conifer Forest	22
Temperate Broad-leaved Forest	21
Semi-Arid Woodland	16
Boreal Conifer	7
Grassland	7
Crop	6
Alpine	6
Arctic	4
Tropical Forest	3
Mixed Forest	3
Boreal Broad-leaved Forest	1
Wetland	1

Table 6.2 The suite of measurements collected at FLUXNET sites and needed for SVAT modeling activity.

Variable	Symbol	Unit	Frequency	Criticality
Mass and Energy Flux Densities				
CO_2	F_c	μmol m^{-2} s^{-1}	1- 2 $hour^{-1}$	core
CO_2 Storage		μmol m^{-2} s^{-1}	1- 2 $hour^{-1}$	core
Latent heat (water vapor)	λE	W m^{-2}	1- 2 $hour^{-1}$	core
Sensible heat	H	W m^{-2}	1- 2 $hour^{-1}$	core
Soil heat conduction	G	W m^{-2}	1- 2 $hour^{-1}$	core
Canopy heat storage	S	W m^{-2}	1- 2 $hour^{-1}$	core
Momentum		kg m^{-1} s^{-2}	1- 2 $hour^{-1}$	core
dry deposition of N		kg ha^{-1} y^{-1}	annual	desired
Meteorology				
Global Radiation	R_g	W m^{-2}	1- 2 $hour^{-1}$	core
Net Radiation	R_n	W m^{-2}	1- 2 $hour^{-1}$	core
Photosynthetic Photon Flux Density	Q_p	μmol m^{-2} s^{-1}	1- 2 $hour^{-1}$	core
Diffuse Radiation		μmol m^{-2} s^{-1} or W m^{-2}	1-2 $hour^{-1}$	desired
Air Temperature	T_a	^oC	1- 2 $hour^{-1}$	core
Humidity			1- 2 $hour^{-1}$	core
CO_2 Concentration	$[CO_2]$	μmol mol^{-1}	1- 2 $hour^{-1}$	core
Wind Speed	U	m s^{-1}	1- 2 $hour^{-1}$	core
Wind Direction		degree	1- 2 $hour^{-1}$	core
Precipitation			daily	core
Pressure	P	kPa	hourly to daily	desired
canopy wetness			hourly	desired
pollution (O_3, NO_2, NO, SO_2)		ppb	hourly	desired
bole temperature	T_b	^oC	1- 2 $hour^{-1}$	core
Light Transmission		μmol m^{-2} s^{-1}	1- 2 $hour^{-1}$	desired
Soil Characteristics				
Soil Temperature Profiles	T_s	^oC	1- 2 $hour^{-1}$	core
Soil Moisture			daily to weekly	core
bulk density			once	core
soil texture			once	core
root depth			once	core
CO_2 efflux		μmol m^{-2} s^{-1}	hourly to seasonally	core/desired
Litter decomposition			annually	core/desired
Litter Chemistry (C, N, Lignin)			annual	desired
Soil (C, N)			annual	desired
Soil Thermal Conductivity			once	desired
Soil hydraulic Conductivity			once	desired
Cation Exchange Capacity			once	desired
Vegetation Characteristics				
Species Composition			once	core
Above Ground Biomass			once	core
Leaf Area Index			seasonal to annual	core
Canopy Height	H	m	seasonal to annual	core
Albedo				
Aerodynamic roughness length	z_o	m	once	desired
zero plane displacement	D	m	once	desired
multi-spectral image			annual	desired
above ground growth increment			annual	core
leaf N and C			seasonal	core
specific leaf weight			seasonal	core
Eco-physiology				
Photosynthetic capacity	V_{cmax}, J_{max}	μmol m^{-2} s^{-1}	weekly to seasonally	desired
pre-dawn water potential	ψ	MPa	weekly to seasonally	desired
stomatal conductance	g_s	mol m^{-2} s^{-1}	weekly to seasonally	desired
tissue $^{13}C/^{12}C$				
Atmospheric $^{13}C/^{12}C$				
sap flow		mol m^{-2} s^{-1}	hourly	desired

Table 6.3: The following AMERIFLUX sites will be used in our initial near real-time validation of MODIS net primary production algorithm:

1. Barrow - tundra - Alaska - 70°18´ N, 156°36´ W
2. Happy Valley - tundra - Alaska - 69°06´ N, 148°48´ W
3. U Pad - tundra - Alaska - 70°16´ N, 148°54´ W
4. Blodgett Forest - Ponderosa pine - California - 38°53´ N, 120°37´ W
5. Jasper Ridge - natural C3 low profile (serpentine grassland) - California - 37°24´ N, 122°3´ W
6. Sky Oaks - chaparral - California - 33°22´ N, 116°37´ W
7. Niwot Ridge - second growth (95 yrs) subalpine forest - Colorado - 40°01´57´´ N, 105°32´49´´ W
8. Natural cypress wetland - Florida - 29°44´ N, 82°05´ W
9. Slash Pine Plantation - Florida - 29°44´ N, 82°05´ W
10. Bondville -crops - Illinois - 40°0.366´ N, 88°17.512´ W
11. Morgan Monroe State Forest - deciduous - Southern Indiana - 39°19´ N, 86°25´ W
12. Konza Prairie - natural, low profile C4 prairie - Kansas - 39°07´ N, 94°21´ W
13. Walnut River Watershed - C3/C4 prairie to tall grass- Kansas - 37°31´15´´ N, 96°51´18´´ W
14. Harvard Forest - deciduous - Massachusetts - 42°32´ N, 72°11´ W
15. Smithsonian Environmental Research Center (SERC) - mostly deciduous forest - Maryland - 38°53´ N 76°33´ W
16. Howland Forest - old coniferous - Maine - 45°15´ N, 68°45´ W
17. Northern Michigan Site - mid-aged mostly deciduous forest - Michigan - 45°35´ N, 84°42´W
18. Duke Forest - even-aged loblolly pine forest site and a second growth uneven-aged, multi-species deciduous site - North Carolina - 35°52´ N, 79°59´ W
19. Little Washita Watershed - rangeland - Oklahoma - 34°57.624´ N, 97°58.7337´ W
20. Ponca City - Agricultural Wheat - Oklahoma -36°45´ N, 97°05´ W
21. Shidler - Native Tallgrass Prairie - Oklahoma - 36°51´ N, 96°41´ W
22. Juniper Site - juniper/sagebrush - Oregon - 44°15´54´´ N, 121°23´3´´ W
23. Metolius Research Natural Area - open ponderosa pine (old/young patches) - Oregon - 44°29´56´³ N, 121°37´26´´ W
24. Temperate Coniferous - 15-yr old ponderosa pine, natural regeneration - Oregon - 44°25´ N, 121°34´ W
25. Walker Branch - deciduous - Tennessee - 35°57´30´´ N, 84°17´15´´ W
26. Wind River Crane Site - old coniferous - Washington State - 45°49´ N, 121°58´ W
27. Park Falls - boreal lowland and wetland forest - Wisconsin - 45°56´43´´ N, 90°16´28´´ W
28. Glacier Lake Ecosystem Experiments Site - subalpine/alpine (Engelman spruce and Subalpine fir) - Wyoming - 41°20´ N, 106° 20´ W

7. REFERENCES

Aber, J.D., Melillo, J.M., Nadelhoffer, K.J., Pastor, J. and Boone, R.D., 1991. Factors controlling nitrogen cycling and nitrogen saturation in northern temperate forest ecosystems. Ecological Applications, 1(3): 303-315.

Asrar, G., Fuchs, M., Kanemasu, E.T. and Hatfield, J.H., 1984. Estimating absorbed photosynthetic radiation and leaf area index from spectral reflectance in wheat. Agronomy Journal, 76: 300-306.

Asrar, G., Myneni, R.B. and Choudhury, B.J., 1992. Spatial heterogeneity in vegetation canopies and remote sensing of absorbed photosynthetically active radiation: a modeling study. Remote Sensing of Environment, 41: 85-103.

Baldocchi, D., Hicks, B.B. and Meyers, T.P., 1988. Measuring biosphere-atmosphere exchanges of biologically related gases with micrometeorological methods. Ecology, 69: 1331-1340.

Baldocchi, D., Valentini, R., Running, S., Oechel, W. and Dahlman, R., 1996. Strategies for measuring and modeling carbon dioxide and water vapour fluxes over terrestrial ecosystems. Global Change Biology, 2: 159-168.

Benson, B.J. and MacKenzie, M.D., 1995. Effects of sensor spatial resolution on landscape structure parameters. Landscape Ecology, 10: 113-120.

Beringer, F., 1994. Simulated irradiance and temperature estimates as a possible source of bias in the simulation of photosynthesis. Agricultural and Forest Meteorology, 71: 19-32.

Cannell, M.G.R., 1982. World Forest Biomass and Primary Production Data. Academic Press, London, 391 pp.

Churkina, G. and Running, S.W., 1998. Contrasting climatic controls on the estimated productivity of global terrestrial biomes. Ecosystems, 1: 206-215.

Cienciala, E., Running, S.W., Lindroth, A., Grelle, A. and Ryan, M.G., 1998. Analysis of carbon and water fluxes from the NOPEX boreal forest: comparison of measurements with FOREST-BGC simulations. Journal of Hydrology, 212-213: 62-78.

Cohen, W.B., Fiorella, M., Gray, J., Helmer, E. and Anderson, K., 1998. An efficient and accurate method for mapping forest clearcuts in the Pacific Northwest using Landsat imagery. Photogrammetric Engineering and Remote Sensing, 64: 293-300.

Cohen, W.B., Spies, T.A. and Fiorella, M., 1995. Estimating the age and structure of forests in a multi-ownership landscape of western Oregon. International Journal of Remote Sensing, 16: 721-746.

Cramer, W. et al., 1999. Comparing global models of terrestrial net primary productivity (NPP): Overview and key results. Global Change Biology, in press.

Dang, Q.-L., Margolis, H.A., Coyea, M.R., Sy, M. and Collatz, G.J., 1997. Regulation of branch-level gas exchange of boreal trees: roles of shoot water potential and vapor pressure difference. Tree Physiology, 17: 521-535.

Davies, W.J. and Zhang, J., 1991. Root signals and the regulation of growth and development of plants in drying soil. Annual Reviews of Plant Physiology and Plant Molecular Biology, 42: 55-76.

Dentener, F.J. and Crutzen, P.J., 1994. A three-dimensional model of the global ammonia cycle. Journal of Atmospheric Chemistry, 19: 331-369.

Dickinson, R.E., 1995. Land processes in climate models. Remote Sensing of Environment, 51: 27-38.

Ellsworth, D.S. and Reich, P.B., 1993. Canopy structure and vertical patterns of photosynthesis and related leaf traits in a deciduous forest. Oecologia, 96: 169-178.

Evans, J.R., 1989. Photosynthesis and nitrogen relationships in leaves in C_3 plants. Oecologia, 78: 9-19.

Fahey, T.J., Yavitt, J.B. and Pearson, J.A., 1985. The nitrogen cycle in lodgepole pine forests, southeastern Wyoming. Biogeochemistry, 1: 257-275.

Fan, S.-M. et al., 1995. Environmental controls on the photosynthesis and respiration of a boreal lichen woodland: a growing season of whole-ecosystem exchange measurements by eddy correlation. Oecologia, 102: 443-452.

Frolking, S. et al., 1996. Modeling temporal variability in the carbon balance of a spruce/moss boreal forest. Global Change Biology, 2: 343-366.

Global Climate Observing System, 1997. GCOS/GTOS plan for terrestrial climate-related observations. Ver 2.0. GCOS-32, QMO/TD-No. 796, World Meteorological Organization.

Goulden, M.L., Munger, J.W., Fan, S.-M., Daube, B.C. and Wofsy, S., 1996. Exchange of carbon dioxide by a deciduous forest: response to interannual climate variability. Science, 271: 1576-1578.

Goward, S.N., Tucker, C.J. and Dye, D.G., 1985. North American vegetation patterns observed woth the NOAA-7 Advanced Very High Respolution Radiometer. Vegetatio, 64: 3-14.

Hanan, N.P., Prince, S.D. and Bégué, A., 1997. Modelling vegetation primary production during HAPEX-Sahel using production efficiency and canopy conductance model formulations. Journal of Hydrology, 188-189: 651-675.

Hikosaka, K., Terashima, I. and Katoh, S., 1994. Effects of leaf age, nitrogen nutrition and photon flux density on the distribution of nitrogen among leaves of a vine (*Ipomoea tricolor* Cav.) grown horizontally to avoid mutual shading of leaves. Oecologia, 97: 451-457.

Hirose, T. and Werger, M.J.A., 1994. Photosynthetic capacity and nitrogen partitioning among species in the canopy of a herbaceous plant community. Oecologia, 100: 203-212.

Holland, E.A. et al., 1997. Variation in the predicted spatial distribution of atmospheric nitrogen deposition and their impact on carbon uptake by terrestrial ecosystems. Journal of Geophysical Research, 102(D13): 15849-15866.

Hollinger, D.Y. et al., 1994. Carbon dioxide exchange between an undisturbed old-growth temperate forest and the atmosphere. Ecology, 75: 134-150.

Hudson, R.J.M., Gherini, S.A. and Goldstein, R.A., 1994. Modeling the global carbon cycle: nitrogen fertilization of the terrestrial biosphere and the "missing" CO_2 sink. Global Biogeochemical Cycles, 8(3): 307-333.

Hunt, E.R., Jr., 1994. Relationship between woody biomass and PAR conversion efficiency for estimating net primary production from NDVI. International Journal of Remote Sensing, 15: 1725-1730.

Hunt, E.R., Jr. et al., 1996. Global net carbon exchange and intra-annual atmospheric CO_2 concentrations predicted by an ecosystem process model and three-

dimensional atmospheric transport model. Global Biogeochemical Cycles, 10(3): 431-456.

Jackson, R.D., Slater, P.N. and Pinter, P.J., Jr., 1983. Discrimination of growth and water stress in wheat by various vegetation indices through clear and turbid atmospheres. Remote Sensing of Environment, 13: 187-208.

Justice, C.O. et al., 1998. The moderate resolution imaging spectroradiometer (MODIS): land remote sensing for global change research. IEEE Transactions on Geoscience and Remote Sensing, 36(4): 1228-1249.

Keeling, C.D., Chin, J.F.S. and Whorf, T.P., 1996. Increased activity of northern vegetation inferred from atmospheric CO_2 measurements. Nature, 382: 146-149.

Kimball, J.S., Running, S.W. and Nemani, R., 1997a. An improved method for estimating surface humidity from daily minimum temperature. Agricultural and Forest Meteorology, 85: 87-98.

Kimball, J.S., Thornton, P.E., White, M.A. and Running, S.W., 1997b. Simulating forest productivity and surface-atmosphere exchange in the BOREAS study region. Tree Physiology, 17: 589-599.

Kimball, J.S., White, M.A. and Running, S.W., 1997c. BIOME-BGC simulations of stand hydrologic processes for BOREAS. Journal of Geophysical Research, 102(D24): 29043-29051.

Kittel, T.G.F., Rosenbloom, N.A., Painter, T.H., Schimel, D.S. and VEMAP Modelling Participants, 1995. The VEMAP integrated database for modelling United States ecosystem/vegetation sensitivity to climate change. Journal of Biogeography, 22: 857-862.

Landsberg, J.J. and Gower, S.T., 1997. Applications of Physiological Ecology to Forest Management. Physiological Ecology Series. Academic Press, San Diego, CA.

Landsberg, J.J. et al., 1996. Energy coversion and use in forests: The analysis of forest production in terms of radiation utilisation efficiency. In: H.L. Gholz and K. Nakane (Editors), The Use of Remote Sensing in the Modeling of Forest Productivity at Scales from the Stand to the Globe. Kluwer Academic Press, London.

Larcher, W., 1995. Physiological Plant Ecology. Springer-Verlag, Berlin Heidelberg.

Lavigne, M.B. and Ryan, M.G., 1997. Growth and maintenance respiration rates of aspen, black spruce, and jack pine stems at northern and southern BOREAS sites. Tree Physiology, 17: 543-551.

Lenschow, D.H., 1995. Micrometeorological techniques for measuring biosphere-atmosphere trace gas exchange. In: P. Matson and B. Harris (Editors), Methods in Ecology: Trace Gases. ??, ??, pp. ??

Maier, C.A., Zarnoch, S.J. and Dougherty, P.M., 1998. Effects of temperature and tissue nitrogen on dormant season stem and branch maintenance respiration in a young loblolly pine (*Pinus taeda*) plantation. Tree Physiology, 18: 11-20.

Meinzer, F.C. et al., 1995. Environmental and physiological regulation of transpiration in tropical forest gap species: the influence of boundary layer and hydraulic properties. Oecologia, 101: 514-552.

Moncrieff, J.B., Malhi, Y. and Leuning, R., 1996. The propogation of errors in long-term measurements of land-atmosphere fluxes of carbon and water. Global Change Biology, 2: 231-240.

Monteith, J.L., 1972. Solar radiation and productivity in tropical ecosystems. Journal of Applied Ecology, 9: 747-766.

Monteith, J.L., 1977. Climate and efficiency of crop production in Britain. Philosophical Transactions of the Royal Society of London, Ser. B: 277-294.

Moore, C.J., 1986. Frequency response corrections for eddy correlation systems. Boundary Layer Meteorology, 37: 17-35.

Pataki, D.E., Oren, R., Katul, G. and Sigmon, J., 1998. Canopy conductance of *Pinus taeda*, *Liquidambar styraciflua* and *Quercus phellos* under varying atmospheric and soil water conditions. Tree Physiology, 18: 307-315.

Piper, S.C., 1995. Construction and description of a gridded global dataset of daily temperature and precipitation for terrestrial biospheric modelling. S.I.O. Reference Series No. 94-13, Scripps Institute of Oceanography, University of California, San Diego, San Diego.

Potter, C.S. et al., 1993. Terrestrial ecosystem production: a process model based on global satellite and surface data. Global Biogeochemical Cycles, 7(4): 811-841.

Press, W.H., Teukolsky, S.A., Vetterling, W.T. and Flannery, B.P., 1992. Numerical recipes in C: the art of scientific computing. Cambridge University Press.

Prince, S.D., 1991. A model of regional primary production for use with coarse resolution satellite data. International Journal of Remote Sensing, 12: 1313-1330.

Prince, S.D. and Goward, S.T., 1995. Global primary production: a remote sensing approach. Journal of Biogeography, 22: 815-835.

Reich, P.B., Kloeppel, B.D., Ellsworth, D.S. and Walters, M.B., 1995. Different photosynthesis-nitrogen relations in deciduous hardwood and evergreen coniferous tree species. Oecologia, 104: 24-30.

Reich, P.B., Walters, M.B., Ellsworth, D.S. and Uhl, C., 1994. Photosynthesis-nitrogen relations in Amazonian tree species. I. Patterns among species and communities. Oecologia, 97: 62-72.

Running, S.W., 1984. Microclimate control of forest productivity: analysis by computer simulation of annual photosynthesis/transpiration balace in different environments. Agricultural and Forest Meteorology, 32: 267-288.

Running, S.W., 1994. Testing FOREST-BGC ecosystem process simulations across a climatic gradient in Oregon. Ecological Applications, 4(2): 238-247.

Running, S.W. and Coughlan, J.C., 1988. A general model of forest ecosystem processes for regional applications.

I. Hydrological balance, canopy gas exchange and primary production processes. Ecological Modelling, 42: 125-154.

Running, S.W. and Hunt, E.R., Jr., 1993. Generalization of a forest ecosystem process model for other biomes, BIOME-BGC, and an applicationfor global-scale models. In: J.R. Ehleringer and C. Field (Editors), Scaling Physiological Processes: Leaf to Globe. Academic Press, San Diego, CA, pp. 141-158.

Running, S.W. et al., 1994. Terrestrial remote sensing science and algorithms planned for EOS/MODIS. International Journal of Remote Sensing, 15(17): 3587-3620.

Running, S.W. et al., 1989. Mapping regional forest evapotranspiration and photosynthesis by coupling satellite data with ecosystem simlation. Ecology, 70(4): 1090-1101.

Russell, G., Jarvis, P.G. and Monteith, J.L., 1989. Absoption of radiation by canopies and stand growth. In: G. Russell, B. Marshall and P.G. Jarvis (Editors), Plant canopies: their growth, form and function. Cambridge University Press, Cambridge, pp. 21-40.

Ryan, M.G., Binkley, D. and Fownes, J.H., 1997. Age-related decline in forest productivity: pattern and process. Advances in Ecological Research, 27: 213-261.

Schimel, D.S., VEMAP Participants and Braswell, B.H., 1997. Continental scale variability in ecosystem processes: Models, data, and the role of disturbance. Ecological Monographs, 67: 251-271.

Schwarz, P.A., Fahey, T.J. and Dawson, T.E., 1997. Seasonal air and soil temperature effects on photosynthesis in red spruce (*Picea rubens*) saplings. Tree Physiology, 17: 187-194.

Sellers, P.J., 1987. Canopy reflectance, photosynthesis and transpiration. II. The role of biophysics in the linearity of their interdependence. Remote Sensing of Environment, 21: 143-183.

Sellers, P.J., Berry, J.A., Collatz, G.J., Field, C.B. and Hall, F.G., 1992. Canopy reflectance, photosynthesis, and transpiration. III. A reanalysis using improved leaf models and a new canopy integration scheme. Remote Sensing of Environment, 42: 187-216.

Sprugel, D.G., Ryan, M.G., Brooks, J.R., Vogt, K.A. and Martin, T.A., 1995. Respiration from the organ level to stand level. In: W.K. Smith and T.M. Hinkley (Editors), Resource Physiology of Conifers. Academic Press, San Diego,CA, pp. 255-299.

Tans, P.P., Bakwin, P.S. and Guenther, D.W., 1996. A feasible global carbon cycle observing system: a plan to decipher today's carbon cycle based on observations. Global Change Biology, 2: 309-318.

Thornton, P.E., 1998. Regional ecosystem simulation: combining surface- and satellite-based observations to study linkages between terrestrial energy and mass budgets. Ph.D. Thesis, The University of Montana, Missoula, 280 pp.

Thornton, P.E. and Running, S.W., 1999. An improved algorithm for estimating incident daily solar radiation from measurements of temperature, humidity, and precipitation. Agricultural and Forest Meteorology, 93: 211-228.

Townshend, J.R.C. and Justice, C.O., 1988. Selecting the spatial resolution of satellite sensors required for global monitoring of land transformations. International Journal of Remote Sensing, 9: 187-236.

VEMAP Members, 1995. Vegetation/Ecosystem Modeling and Analysis Project (VEMAP):Comparing biogeography and biogeochemistry models in a continental-scale study of terrestrial ecosystem responses to climate change and CO_2 doubling. Global Biogeochemical Cycles, 9: 407-437.

Veroustraete, F., Patyn, J. and Myneni, R.B., 1996. Estimating net ecosystem exchange of carbon using the normalized difference vegetation index and an ecosystem model. Remote Sensing of Environment, 58: 115-130.

Waring, R.H. et al., 1995. Scaling gross ecosystem production at Harvard Forest with remote sensing: a comparison of estimates from a constrained quantum-use efficiency model and eddy correlation. Plant, Cell and Environment, 18: 1201-1213.

Waring, R.H. and Running, S.W., 1998. Forest Ecosystems: Analysis at Multiple Scales. Academic Press, San Diego, CA, 370 pp.

White, J.D. et al., 1998. Assessing simulated ecosystem processes for climate variability research at Glacier National Park, USA. Ecological Applications, 8: 805-823.

Will, R.E. and Teskey, R.O., 1997. Effect of elevated carbon dioxide concentration and root restriction in net photosynthesis, water relations and foliar carbohydrate status of loblolly pine seedlings. Tree Physiology, 17: 655-661.

Zobler, L., 1986. A world soil file for global climate modeling. Tech. Memo 87802, NASA, Greenbelt, MD.